Causal Mixture Models: Characterization and Discovery

Sarah Mameche
CISPA Helmholtz Center
for Information Security
sarah.mameche@cispa.de

Janis Kalofolias
CISPA Helmholtz Center
for Information Security
janis.kalofolias@cispa.de

Jilles Vreeken
CISPA Helmholtz Center
for Information Security
jv@cispa.de

Abstract

Real-world datasets are often a combination of unobserved subpopulations that follow distinct causal generating processes. In an observational study, for example, participants may fall into unknown groups that either (a) respond effectively to a drug, or (b) show no response due to drug resistance. Not accounting for such heterogeneity then risks biased estimates of drug effectiveness. In this work, we formulate this setting through a causal mixture model, in which the data-generating process of each variable depends on latent group membership (a or b). Specifically, we model each variable as a mixture of structural causal equation models, where latent categorical (mixing) variables index assignment to subpopulations. Unlike prior work, the approach allows for multiple independent mixing variables, each affecting distinct sets of observed variables. To infer both the graph, mixing variables, and assignments jointly, we integrate mixture modeling into score-based causal discovery; show theoretically that the resulting scoring criterion is consistent; and demonstrate empirically that the resulting causal discovery approach discovers the causal model in synthetic and real-world evaluations.

1 Introduction

A central part of scientific investigation is understanding cause-effect relationships, which the field of causal discovery [Pearl, 2009] aims to discover directly from observational data. Many existing causal discovery approaches, however, rely on idealized assumptions, among others assuming that no relevant unmeasured variables exist and that all samples come from a homogeneous distribution. Real-world applications might violate both assumptions, for example, when observations come from heterogeneous populations or environments.

Take, for example, a nationwide study of antimicrobial resistance in hospitalized patients, focusing on a resistant pathogen such as Methicillin-Resistant Staphylococcus Aureus (MRSA) [Hasanpour et al., 2023]. As patients come from different regions, their individual medical histories differ, including prior exposure to pathogens such as Enterococcus [Li et al., 2022] with known cross-resistance to MRSA. The regional plasmid profiles of Enterococcus largely determine its susceptibility, say to Vancomycin [Boumasmoud et al., 2022], in turn influencing MRSA cross-resistance [Arredondo-Alonso et al., 2020]. Although well documented, this variable is not routinely measured, and is hence a latent variable that defines the mechanism under which the presence of Enteroccocus affects MRSA cross-resistance [Cong et al., 2019]. Consequently, observations across regions effectively arise from a mixture of distinct causal mechanisms.

More generally, observational data can be a combination of multiple subgroups with distinct generating processes. To illustrate, consider a simplified, synthetic setting in Fig. 1, where the causal mechanism for Y is a mixture of two functional relationships $X \to Y$. Treating all samples as one population can then cause artifacts during causal discovery, such as spurious relationships or reversed

39th Conference on Neural Information Processing Systems (NeurIPS 2025).

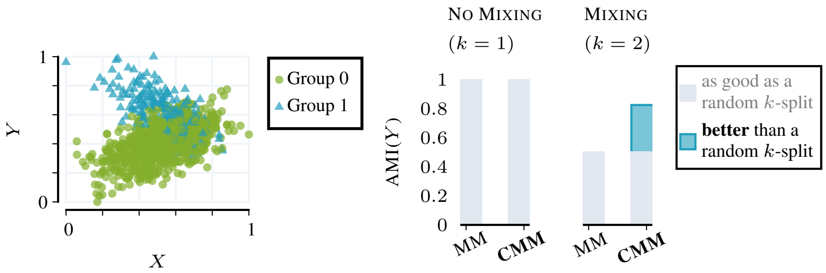

Figure 1: *Causal Mixture Models.* Left: Example of a mixed causal relationship $X \rightarrow Y$. Right: Recovering the class assignments with (Gaussian) mixture models (MM) compared to causal mixture models (CMM) on simulated bivariate datasets.

causation [Huang et al., 2020]. While a line of research known as multi-context and interventional causal discovery [Mooij et al., 2016; Huang et al., 2020; Squires et al., 2020] addresses a similar setting, these require access to multiple datasets where all causal mechanisms remain fixed, which are unknown in the motivating example.

Recent works attempt to separate a single given dataset into multiple interventional datasets or environments; for instance, Kumar et al., 2024 combine Gaussian mixture modeling (GMM) with interventional discovery (UT-IGSP), addressing . mixtures arising from atomic interventions [Kumar et al., 2024]. In examples such as Fig. 1, the underlying mixtures are better captured through conditional relationships, such as in mixture-of-regressions models [Hennig, 2000]. To illustrate the difference between an unconditional mixture model (MM) and the conditional (causal) counterpart (CMM), we draw synthetic datasets over X, Y and evaluate the discovered class assignments for Y via the Adjusted Mutual Information (AMI). While in the case without mixing ($k = 1$ group), both methods correctly reject the existence of groups, with mixing ($k = 2$ groups), the MM reports no better than random assignments, whereas the CMM improves over the baseline. This suggests considering the causal mechanism for Y as a conditional mixture subject to a latent variable Z.

When extending the scope from the bivariate case to multiple observed variables, our interest then also extends from a single to multiple, independent latent variables. Returning to the motivating example, for instance, suppose each medical center chooses a different collaborating laboratory for antibiotic testing. This introduces a batch effect, a latent factor independent of regional susceptibility. To address this, different from previous formalizations that assume a single mixing variable affecting all observables [Mazaheri et al., 2023; Kumar et al., 2024], we allow multiple independent mixing variables that each affect different subsets of observed variables (cf. Fig. 2). For each variable, we model its generating mechanism as a conditional mixture given its direct causes and its corresponding latent factor, referred to as a Causal Mixture Model (CMM). The central question in the remainder of this work is how to infer the structure of such models from data.

Causal Mixture Models To summarize, we propose basing mixture modeling on functional relationships within a causal graph, where we consider the causal mechanism for each variable as a mixture of conditional relationships given its causes and an associated latent variable. Unlike two-stage approaches that separate cluster and graph discovery, our approach integrates mixture inference directly into causal discovery by extending local score-based criteria, where we focus on linear mixture-of-regression (MLR) models inferred through Expectation Maximization (EM) and extend the BIC score [Chickering, 2002]. We show that under oracle access to the MLR parameters, we can guarantee the identification of the causal model under mild assumptions, and hypothesize that this also holds for their EM estimates in practice. We propose integrating this approach into score-based causal discovery algorithms such as Greedy Equivalence Search (GES) [Chickering, 2002] or TOPIC [Xu et al., 2025]. To demonstrate empirically we can recover the CMM components in practice, we consider simulated mixed data, a mixture of interventions [Kumar et al., 2024], as well as a real-world benchmark on causal cell signaling pathways [Sachs et al., 2005].

We include all theoretical justifications and experimental details in the supplement.

2 Causal Model

Given a set of continuous random variables $\boldsymbol{X} = \{X_1, \dots, X_n\}$, we are interested not only in causal relationships among them, but especially in unknown changes of their causal mechanisms. Assuming that the mechanisms are linear functions of a fixed subset of the observed random variables, we allow their coefficients to be chosen from a finite set of vectors conditional on an external latent variable.

To formalise this, we also consider a set of discrete, unobserved random variables $\boldsymbol{Z} = \{Z_1, \dots, Z_m\}$, with $m \leq n$, each following a categorical distribution $Z_i \sim \mathrm{Categorical}(\boldsymbol{\gamma}^i)$ with $Z_i \in \{1, \dots, K_i\}$. That is, each $\boldsymbol{\gamma}^i$ lies on a K_i-dimensional probability simplex $\boldsymbol{\gamma}^i = (\gamma^i_1, \dots, \gamma^i_{K_i})$ with $\sum_{k=1}^{K_i} \gamma^i_k = 1$, so that $\mathbb{P}(Z_i = k) = \gamma^i_k$. We call these random variables *mixing variables*.

The causal mechanism of each observed random variable in $\boldsymbol{X}$ depends, besides on the set of observed causal parents denoted $\mathbf{Pa}_j$, on exactly one of the unobserved, latent $\boldsymbol{Z}$, as determined by the surjective map $\mathrm{La} : \boldsymbol{X} \to \boldsymbol{Z} : X_j \mapsto Z_i$, in which case we simply write $\mathrm{La}_j = Z_i$. The mixing variable directly affects the parameters of the causal mechanism, which we therefore express as a function $b_j : [K_i] \to \mathbb{R}^{|\mathbf{Pa}_j|} : z \mapsto \beta_{jz}$ mapping each value z of Z_i to a linear coefficient vector $\beta_{jz} \in \mathbb{R}^{|\mathbf{Pa}_j|}$. Hence, the parameters of the functional dependency f is the collection of vectors $B_j = (\beta_{j1}, \dots, \beta_{jK_i})$; this consists of one coefficient vector β_{jk} for each mixing coefficient $1 \leq k \leq K_i$, and each such vector has dimension equal to the number of parents $\mathbf{Pa}_j$ of X_j.

Summarizing, we can now model each random variable X_j as generated from its observed causes $\mathbf{Pa}_j \subseteq \boldsymbol{X}$ by the causal function f and the coefficients b_j that depend on the latent $Z_i = \mathrm{La}_j \in \boldsymbol{Z}$, where we recall that $\boldsymbol{Z} \cap \boldsymbol{X} = \emptyset$. Then, we have

$$X_j = f(\mathbf{Pa}_j, b_j) + N_j \qquad \text{with} \qquad f(x, b_j(z)) = \beta_{jz}^\top x + \beta_{jz}^{(0)}, \tag{1}$$

where $N_j \perp\!\!\!\perp \mathbf{Pa}_j$ is additive Gaussian noise, $N_j \sim \mathcal{N}(0, \sigma^2)$.

This construction implies that for a random variable X_j for which $\mathrm{La}_j = Z_i$ we get

$$(X_j | \mathbf{Pa}_j = \mathbf{y}, \mathrm{La}_j = k) \sim \mathcal{N}\left(\boldsymbol{\beta}_{jk}{}^\top \mathbf{y}, \sigma^2\right) \qquad \text{for } k \in \{1, \dots, K_i\} \text{ and} \tag{2}$$

$$(X_j | \mathbf{Pa}_j = \mathbf{y}) \qquad \sim \mathrm{MLR}\left(\mathbf{B}_j, \boldsymbol{\gamma}^j, \sigma^2\right) \ , \tag{3}$$

where $\mathrm{MLR}\left(\mathbf{B}, \boldsymbol{\gamma}, \sigma^2\right)$ is the conditional distribution of a mixture of linear regressions with density

$$p^{\mathrm{MLR}}_{X|\mathbf{Y}}(x, \mathbf{y}; \mathbf{B}, \boldsymbol{\gamma}, \sigma^2) = \sum_{k=1}^{K} \gamma_k p^{\mathcal{N}}_X(x; \boldsymbol{\beta}_k{}^\top \mathbf{y}, \sigma^2) = \sum_{k=1}^{K} \frac{\gamma_k}{\sqrt{2\pi}\sigma} \exp\left(-\frac{\|\boldsymbol{\beta}_k{}^\top \mathbf{y} - x\|^2}{2\sigma^2}\right) \ , \tag{4}$$

and $p^{\mathcal{N}}_X(x; \mu, \sigma^2)$ is the density of the normal distribution with mean μ and variance σ^2. Note that in case $\mathbf{Pa}_j = \emptyset$, the formulation reduces to a standard unconditional GMM.

Graphical Model We represent the above causal model as a Directed Acyclic Graph (DAG) $\mathcal{G}^Z = (\boldsymbol{X} \cup \boldsymbol{Z}, E^Z)$ over both observed $\boldsymbol{X}$ and latent $\boldsymbol{Z}$ random variables, between which we add edges $X_j \to X_l$ whenever X_j is a cause of X_l, as well as $Z_i \to X_j$ whenever $\mathrm{La}_j = Z_i$; since the $\boldsymbol{Z}$ were assumed exogenous and independent, we allow no incoming edges toward the $\boldsymbol{Z}$ themselves. Of special interest is the subgraph $\mathcal{G} = (\boldsymbol{X}, E)$ that is induced on $\mathcal{G}^Z$ by the node subset $\boldsymbol{X}$, with $E = \{X_j \to X_l \mid X_j \to X_l \in E^Z\}$. Considering only the latter subgraph, we denote the set of all observed direct predecessors of X_j in $\mathcal{G}$ by $\mathbf{Pa}_j \subset \boldsymbol{X} \setminus \{X_j\}$. We also consider a surjective map $\pi : \boldsymbol{X} \to \mathbb{N}$ which induces a topological ordering on $\mathcal{G}$ (and thus partial ordering over $\boldsymbol{X}$) that we call a *causal order* under $\mathcal{G}$, and assigns such values on $\boldsymbol{X}$ that $X_r \in \mathbf{Pre}_j \Rightarrow \pi(j) < \pi(r)$, for $\mathbf{Pre}_j \subset \boldsymbol{X} \setminus \{X_j\}$ the set of all direct and indirect predecessors of X_j in $\mathcal{G}$. Fig. 2 depicts an example of such a graph $\mathcal{G}^Z$ (colored and black) and the resp. induced subgraph $\mathcal{G}$ (black). We then model edges such as $Z_1 \to X_1$ where X_1 is a source node of the causal graph as a GMM and edges such as $Z_1 \to X_2$ through an MLR.

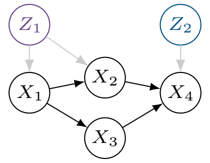

Figure 2: *Example Causal Mixture Model.* The observed variables are affected by two latent mixing variables Z_1, Z_2.

We assume the causal Markov Property to hold in the full causal model $\mathcal{G}^Z$, which results in the following factorization over the observed variables.

Assumption 1 (Mixture-Markov Property)**.** The distribution of $\boldsymbol{X}$ has (marginal) density

$$p_{\boldsymbol{X}}(\mathbf{x}) = \prod_{X_j \in \boldsymbol{X}} p^{\mathrm{MLR}}_{X|\mathbf{Pa}_j}(x, \mathbf{pa}_j; \mathbf{B}, \boldsymbol{\gamma}, \sigma^2) \ , \tag{5}$$

where we implicitly use the independence of all $\boldsymbol{Z}$ (see Appendix A.3 on relaxing this assumption).

The objective in this work is to infer the CMM from finite observations, as follows.

Problem 1. *Given i.i.d. observations $\mathcal{D} = \{\mathbf{x}_1, \ldots, \mathbf{x}_r\}$, of the random variables $\boldsymbol{X}$ generated from a distribution compatible with our assumptions, we aim to infer the structure of $\mathcal{G}^Z$,*

1. *the causal dependencies $X_j \to X_l \in E$ encoded in the edges E of the induced graph $\mathcal{G}$,*
2. *the linear coefficients of the corresponding causal mechanisms $\boldsymbol{\gamma}^j$ for all $X_j \in \boldsymbol{X}$,*
3. *the set $\boldsymbol{Z}$ of latent variables, i.e., their number m, and for each $Z_i \in \boldsymbol{Z}$ the domain K_i and mixing probabilities $\boldsymbol{\gamma}^i$, as well as*
4. *the mapping $\mathrm{La}_j \in \boldsymbol{Z}$ for each $X_j \in \boldsymbol{X}$.*

We address this problem in the following section.

3 Theory

As the first contribution of our work, we study conditions that allow inference on $\mathcal{G}^Z$, as formalised in Problem 1, using score-based causal discovery. To this end, it is of interest to determine whether existing local scoring criteria can be adapted for our setting, so as to use them consistently in a score-based framework, such as the well-known Greedy Equivalent Search (GES) algorithm [Chickering, 2002] and related approaches [Xu et al., 2025].

GES performs a greedy search over the set of all Markov equivalent classes (MECs) of causal graphs with nodes $\boldsymbol{X}$. More specifically, each iteration updates the current MEC by the best hypothesis among all those that differ from the current one by a single edge modification (i.e., edge reversal, addition, or removal). This process allows for the inference of the most likely MEC, as expressed in the form of the edges of a Partially Directed Acyclic Graph (PDAG) with nodes representing the observed $\boldsymbol{X}$.

Importantly, GES can be shown to be asymptotically consistent as long as the search is guided by a scoring criterion that satisfies the appropriate criteria given shortly. We write $\mathcal{L}_{\boldsymbol{X}} \in I_{\mathcal{G}}$ for a graph with nodes $\boldsymbol{X}$ whenever the (conditional) independencies implied by the PDAG $\mathcal{G}$ are also true for the distribution $\mathcal{L}_{\boldsymbol{X}}$.

Definition 3.1 (Consistent Scoring Criterion [Chickering, 2002])**.** Given data $\mathcal{D}$ of size r sampled from distribution $\mathcal{L}_{\boldsymbol{X}}$ and two graph hypotheses $\mathcal{G}^{\mathrm{h}}_1$, $\mathcal{G}^{\mathrm{h}}_2$ then the score S is consistent whenever

1. $\mathcal{L}_{\boldsymbol{X}} \in I_{\mathcal{G}^{\mathrm{h}}_1}$ and $\mathcal{L}_{\boldsymbol{X}} \notin I_{\mathcal{G}^{\mathrm{h}}_2} \implies S(\mathcal{G}^{\mathrm{h}}_1; \mathcal{D}) > S(\mathcal{G}^{\mathrm{h}}_2; \mathcal{D})$
2. $\mathcal{L}_{\boldsymbol{X}} \in I_{\mathcal{G}^{\mathrm{h}}_1} \cap I_{\mathcal{G}^{\mathrm{h}}_2}$ and $\mathcal{G}^{\mathrm{h}}_1$ has fewer parameters than $\mathcal{G}^{\mathrm{h}}_2$ it is $S(\mathcal{G}^{\mathrm{h}}_1; \mathcal{D}) > S(\mathcal{G}^{\mathrm{h}}_2; \mathcal{D})$.

One score that satisfies this criterion is the Bayes Information Criterion (BIC).

Definition 3.2 (Bayes Information Criterion)**.** Given model hypothesis $\mathcal{H}$ assuming distribution $\mathcal{L}_{\boldsymbol{X}}(\boldsymbol{\theta})$ with parameters $\boldsymbol{\theta} \in \Theta \subseteq \mathbb{R}^d$ and observations $\mathcal{D} = \{\mathbf{x}_1, \ldots, \mathbf{x}_r\}$ of $\boldsymbol{X}$, the score of $\mathcal{H}$ is

$$\mathrm{BIC}(\mathcal{H}) \coloneqq -2 \log p_{\boldsymbol{X}}(\mathcal{D} | \hat{\boldsymbol{\theta}}) + d \log r \,, \tag{6}$$

where the first term is the scaled (log) likelihood of $\mathcal{L}_{\boldsymbol{X}}$ evaluated at its maximiser $\hat{\boldsymbol{\theta}}$.

This score has the important property of decomposability [Chickering, 2002], dictating that when $\mathcal{L}_{\boldsymbol{X}}$ factorises as a product the BIC decomposes as a sum

$$p_{\boldsymbol{X}}(\mathbf{x}) = \prod_{X_j \in \boldsymbol{X}} p_{X_j|\mathbf{Pa}_j}(x_j | \mathbf{pa}_j) \qquad \implies \qquad \mathrm{BIC}(\boldsymbol{X}) = \sum_{X_j \in \boldsymbol{X}} \mathrm{BIC}(X_j | \mathbf{Pa}_j) \,. \tag{7}$$

To transfer these properties to our own model, we need to further account for the latent mixing variables. Hence, at each step of the GES algorithm, and according to our model of Eq. (5) we need to compute the likelihood $p^{\mathrm{MLR}}_{X|\mathbf{Pa}_j}(x, \mathbf{pa}_j; \mathbf{B}, \boldsymbol{\gamma}, \sigma^2)$, which requires an estimation of the Mixture of

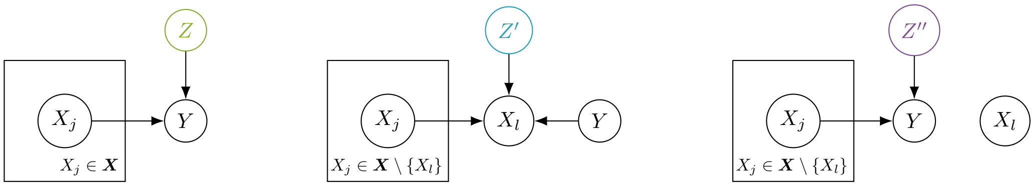
Z
X_j
Y
$X_j \in \boldsymbol{X}$
Z'
X_j
X_l
Y
$X_j \in \boldsymbol{X} \setminus \{X_l\}$
Z''
X_j
Y
X_l
$X_j \in \boldsymbol{X} \setminus \{X_l\}$

Figure 3: *Identifiable Cases.* Under mild assumptions, when Z has at least two mixing components, all of the shown DAGs are identifiable.

Linear Regressions (MLR) parameters. Unfortunately, the computation of the Maximum Likelihood Estimate (MLE) estimates for both Gaussian Mixture Models (GMMs) and MLR models is NP-hard in the general case. However, an efficient algorithm to compute well-performing local maximisers of the corresponding likelihoods is the Expectation Maximisation (EM) framework [Wu, 1983] and its variants [Bishop, 2006]; we therefore employ these algorithms to approximate the MLE parameters.

Although certain conservative claims can be made for the consistency of EM, we postpone them for later on. Instead, for the first part of our analysis we assume the availability of an oracle that can compute the maximum likelihood estimates for the MLR model for a given number of mixtures K,

$$\hat{\boldsymbol{\theta}} = (\hat{\mathbf{B}}, \hat{\boldsymbol{\gamma}}, \hat{\sigma}) = \underset{(\mathbf{B},\boldsymbol{\gamma},\sigma)\in\Theta_K}{\arg\max} \; p^{\mathrm{MLR}}_{X|\mathbf{Y}}(x, \mathbf{y}; \mathbf{B}, \boldsymbol{\gamma}, \sigma^2)\,, \tag{8}$$

where $\Theta_K = (\mathbb{R}^{|\mathbf{Pa}_j|})^K \times \mathcal{S}^{K-1} \times \mathbb{R}_+$ is the space of the model parameters for K mixtures and $\mathcal{S}^K$ the K-dimensional probability simplex. Given the availability of such an oracle, we can adapt the GES algorithm in a way that both preserves its asymptotic consistency and takes into account any possible latent variables. For this, we also incorporate the asymptotically consistent estimation of the number of components K by maximising the BIC score over a set of allowed values $K \leq K_{\max}$. This gives rise to the latent-aware BIC scores

$$\mathrm{BIC}^{\mathrm{ML}}_{\hat{Z}}(\mathcal{H}) = \max_{1\leq K\leq K_{\max}} \mathrm{BIC}^{\mathrm{ML}}_{\hat{Z}}(\mathcal{H}, K) \quad \text{and} \quad \mathrm{BIC}^{\mathrm{EM}}_{\hat{Z}}(\mathcal{H}) = \max_{1\leq K\leq K_{\max}} \mathrm{BIC}^{\mathrm{EM}}_{\hat{Z}}(\mathcal{H}, K)\,, \tag{9}$$

where $\mathrm{BIC}^{\mathrm{ML}}_{\hat{Z}}$ uses the oracle estimate and $\mathrm{BIC}^{\mathrm{EM}}_{\hat{Z}}$ the EM one. By appropriate use of the decomposability property, we can show that the criterion of Def. 3.1 holds for the former score, $\mathrm{BIC}^{\mathrm{ML}}_{\hat{Z}}$.

Note that a known result shows that linear additive Gaussian noise models are not identifiable [Shimizu et al., 2006; Pearl, 2009], in the sense that the graphs $X \to Y$ and $X \leftarrow Y$ are then Markov equivalent. In our general case, however, and under mild conditions (see Lemma B.1), our model deviates from this problematic case enough for the identifiability of all models in Fig. 3 to become possible.

Theorem 3.3 (Local Consistency of $\mathrm{BIC}^{\mathrm{ML}}_{\hat{Z}}$)**.** *Let $\mathcal{D} = \{\mathbf{x}_1, \ldots, \mathbf{x}_r\}$ be observations of random variables $\boldsymbol{X}$, Y, such that $\boldsymbol{X}|Y \sim \mathrm{MLR}\left(\mathbf{B}, \boldsymbol{\gamma}, \sigma^2\right)$, with general parameters $\boldsymbol{\theta}$ (see Lemma B.1). Then, out of the structural hypotheses depicted in Fig. 3 the $\mathrm{BIC}^{ML}_{\hat{Z}}$ score of the ground truth hypothesis $\mathcal{G}^h_{cs}$ is asymptotically larger than any of the alternative ones, $\mathcal{G}^h_{ws}$ and $\mathcal{G}^h_{me}$, almost surely.*

As a corollary, GES with the $\mathrm{BIC}^{\mathrm{ML}}_{\hat{Z}}$ can identify between these models.

Corollary 3.4. *The latent-aware score $\mathrm{BIC}^{ML}_{\hat{Z}}$ is a consistent scoring criterion.*

In our analysis, however, we have yet to address the discrepancy between the $\mathrm{BIC}^{\mathrm{ML}}_{\hat{Z}}$ that we assumed to be tractable, and the one we actually use above, the $\mathrm{BIC}^{\mathrm{EM}}_{\hat{Z}}$ based on the EM algorithm. Of interest is one particular result of Balakrishnan et al. (2017), which shows that for a Euclidean ball around the optimal parameters of the MLR model, the EM algorithm finds the MLE estimate if it is initialised within this ball. The radius of this ball depends on how well the components of each mixture can be separated, and holds both asymptotically and for the finite sample case.

At the same time, we intuit that when the observations do not fit well with an MLR model, the algorithm will fail to find the correct estimate, resulting in an underestimation, $\mathrm{BIC}^{\mathrm{EM}}_{\hat{Z}} \ll \mathrm{BIC}^{\mathrm{ML}}_{\hat{Z}}$. This assumption would steer the GES algorithm away from selecting the said model, which would instead favor the selection of a correct model. We formalise this intuition as follows.

```
Algorithm 1: DISCOVER A CAUSAL MIXTURE MODEL (CMM)
Input: Dataset $\boldsymbol{X}$, max. number of mixture components $K_{\max}$
Output: Set of latent variables $\boldsymbol{Z}$, causal graph $\mathcal{G}^Z$
Initialize $\boldsymbol{Z} \leftarrow \emptyset, \mathcal{G}^Z \leftarrow \emptyset, \mathcal{G} \leftarrow \emptyset, T \leftarrow [\,]$;
// Discover local mixing and graph
while not all nodes are ordered do
    $X_j \leftarrow$ INFERSOURCE$(T, \mathcal{G})$;
    $\mathcal{G} \leftarrow$ EDGEADDITIONS$(X_j, \mathcal{G})$;
    $\mathcal{G} \leftarrow$ EDGEPRUNING$(X_j, \mathcal{G})$;
    for each $k$ in $1, \ldots, K_{\max}$ do
        Using EM, fit $(X_j|\mathbf{Pa}_j = \mathbf{y}) \sim \text{MLR}\left(\mathbf{B}_j, \gamma^j, \sigma^2\right)$ with $k$ components;
    $Z_j \leftarrow$ mixing assignment with best $\text{BIC}^{\text{EM}}_{\hat{Z}} = \max_{1 \le K \le K_{\max}} \text{BIC}^{\text{EM}}_{\hat{Z}}(K)$;
    $T$.APPEND$(X_j)$;
// Infer global mixing
$\boldsymbol{Z}, \mathcal{G}^Z \leftarrow$ INFERMIXING$(\mathcal{G}, \{Z_j\})$;
return $G$, $\boldsymbol{Z}$;
```

Conjecture 3.5. *The latent-aware score* $\text{BIC}^{EM}_{\hat{Z}}$ *is a consistent scoring criterion.*

The analysis justifies the use of the latent-aware score $\text{BIC}^{\text{EM}}_{\hat{Z}}$ in score-based algorithms for consistent structure estimation. Inspired by this, we complement our theoretical results with a practical implementation using the $\text{BIC}^{\text{EM}}_{\hat{Z}}$, which we present and evaluate in the remainder of this work.

4 Algorithm

Here, we outline an algorithm for discovering *i)* the mixing variables $\boldsymbol{Z}$ and *ii)* the causal graph $\mathcal{G}^Z$. Building on the score consistency that our theory establishes, we propose a joint inference procedure that discovers both components within a score-based framework. At each scoring step, we fit an MLR under a given candidate parent set. Choices for the score-based algorithm include, for example, the GES algorithm [Chickering, 2002] or other score-based causal discovery frameworks. As our main proof-of-concept implementation, we describe how to integrate the latent-aware BIC within the topological order-based framework TOPIC [Xu et al., 2025].

Causal Mixture Inference and Scoring Given a node Y with parents $\text{pa}(Y) \subseteq \boldsymbol{X}$, we score the causal relationship using the latent-aware BIC of Eq. (9). That is, the score accounts for an unknown number of mixtures, where the likelihood takes the form of Eq. (4). To compute the BIC in practice, we need to consider each $1 \le k \le K_{\max}$ up to a given hyperparameter $K_{\max}$and use the Expectation Maximisation (EM) [Bishop, 2006] algorithm to obtain estimates for the MLR parameters; finally, we then use the BIC score of the best such k in our algorithm and the corresponding estimates for the rest of the model parameters. In the special case of source nodes, we infer a GMM similarly using EM. Regarding the number of components k, we assume that a reasonably high maximum number of K_{max} is given that caps the number of mixture components. When MLR model selects $K < K_{\text{max}}$, it is (asymptotically) sure that this estimate of K is the true number of mixture coefficients. When $2 \le K_{\text{max}} < K^*$, for K^* the true number of clusters, the causal structure would still be correctly inferred, as the capped MLR would still offer a higher likelihood versus any alternative model.

Causal and Mixing Structure Search We discover the causal DAG $\mathcal{G}$ over the observed $\boldsymbol{X}$ by embedding the above inference step into the TOPIC algorithm. Considering a candidate edge $X \to Y$, we also define the score difference g as the difference in BICs before and after adding X, $g(X, Y; G) = \text{BIC}_Z(Y \mid \text{pa}(Y) \cup \{X\}) - \text{BIC}_Z(Y \mid \text{pa}(Y))$. TOPIC then constructs the DAG in topological order in the following steps.

(i) *Source Identification:* Identify $X_j = \arg\max_X \min_Y [g(X, Y; G) - g(Y, X; G)]$.
(ii) *Edge Additions:* For each $Y \neq X_t$, add an outgoing edge $X_t \to Y$ if $g(X_t, Y; G) > 0$.
(iii) *Edge Pruning:* Remove any redundant incoming edges $Z \to X_t$ using g.

Following this strategy, we discover a topological order T, DAG $\mathcal{G}$ as well as a mixture assignment Z_i for each variable X_j along the topological order. We finally consolidate these. With the reasoning that pairwise estimated Z_i, Z_l exhibit significant overlap when they correspond to the same mixing variable, we measure the similarity of the assignments, here using Adjusted Mutual Information (AMI), and merge variables when the AMI exceeds its expected value [Vinh et al., 2010].

We summarize our approach in Alg. 1.

5 Related Work

Discovering causal graphs from observational data is a well-studied problem. Among constraint-based methods is the PC algorithm [Spirtes et al., 2001] using conditional independence (CI) testing, among score-based approaches is GES [Chickering, 2002] using local scoring criteria [Huang et al., 2018]. Both search over the space of Markov Equivalence classes (MECs) over DAGs. LiNGAM [Shimizu et al., 2006] and Resit [Hoyer et al., 2008] assume non-Gaussianity and independence of regression residuals to orient edges. Cam [Bühlmann et al., 2014] and Score [Rolland et al., 2022]/DAS [Montagna et al., 2023] combine topological order estimators with pruning to discover a DAG, while TOPIC [Xu et al., 2025] uses Bayesian or information-theoretic scores for both steps. Notears [Zheng et al., 2018] frames DAG discovery as a continuous optimization problem. Given the potential variance- resp. R^2-sortability problems of causal discovery benchmarks [Reisach et al., 2021], Reisach et al., 2023 propose simple baselines exploiting these scoring criteria, VarSort and R^{2}Sort. Finally, some works relax the common assumption of causal sufficiency and allow for latent confounding variables, such as FCI [Spirtes et al., 1993]. In comparison, with discrete-valued latent variables and special interest in their inference, our setting is more similar to multiple environments.

Multiple Environments and Interventional Data Towards addressing non-i.i.d. data, several works consider different datasets (called environments, contexts, or interventional datasets) that arise from interventions or causal mechanism shifts, but within which all causal mechanisms are fixed [Schölkopf et al., 2021]. Extensions of common causal discovery algorithms to this setting exist [Mooij et al., 2016; Huang et al., 2020; Squires et al., 2020; Mameche et al., 2023]. Common to these methods is that they consider causal discovery in an augmented graphical model with a single latent variable that can be interpreted as the (known) dataset index, respectively, with intervention variables, allowing identifiability of the causal model up to the interventional MEC (iMEC) [Hauser and Bühlmann, 2013; Wang et al., 2017a]. A different line of work, addressing causal discovery in time series [Runge, 2020], considers discovering temporal regimes with changes in causal mechanism, such as RPCMCI [Saggioro et al., 2020]. This approach differs from ours in that it discovers changes in causal mechanisms along the temporal dimension, assuming a temporal ordering of observations.

Mixture Modeling and Causal Discovery Gaussian Mixture Models as well as their conditional counterparts, Mixtures of Linear Gaussian Regressions, are well studied [McLachlan and Peel, 2000; Hennig, 2000]. The idea of reinterpreting clustering and mixture modeling within a causal framework is not new; most works in this area assume a global mixing variable, also termed a latent-class confounder [Mazaheri et al., 2023]. Some works study for example the bivariate cases [Hu et al., 2018], discrete variables [Mazaheri et al., 2023] and causal inference settings [Kim et al., 2024; Mazaheri et al., 2025]. Most closely related to ours is the work of Kumar et al., 2024 which proposes Mixture-UT-IGSP (MixUTIGSP), combining a GMM with adequate component selection with UT-IGSP. Kumar et al., 2024 give insight into the sample complexity of identifying interventional mixtures, as well as establish identifiability of the iMEC in this setting using the two-stage approach. We will evaluate against this approach in the next section.

Causal Identifiability Methods exist to identify linear additive Gaussian noise models with equal variance, under further conditions, such as non-perfect dependencies, and what is more, also when other constraints are added (e.g., that the coefficients are all less than the unit) [Peters and Bühlmann, 2013]. Our identification results do not rely on these specific assumptions; instead, we base identification on the effects of the latent mixing variables and the asymmetries they introduce in the causal directions. The results are thus independent of the approach of restricting the functional model with further assumptions, and can address scenarios where these assumptions do not hold.

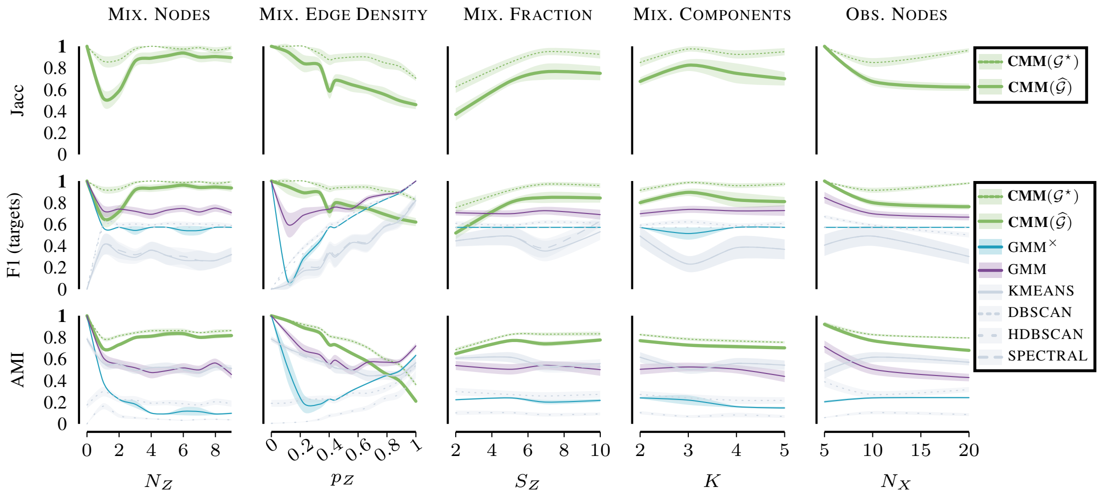

Figure 4: *Discovering Mixing Structure.* In synthetically generated CMMs, we evaluate the quality of the recovered mixing structure, evaluating the affected observed variables (F1 (target)), variable sets affected by the same latent variable (Jacc) as well as per-node mixing assignments (AMI).

6 Evaluation

We evaluate our approach on two main questions,

(i) *Discovering Mixing Structure*: Given a causal graph, can our approach accurately discover the underlying mixing structure, including the number of mixing variables, the number of their components, assignments, and sets of targeted observed variables?

(ii) *Discovering Causal Structure*: When the causal graph is unknown, can our approach recover the mixing structure as well as the causal graph?

We address the above questions on synthetic and real-world data.

Experimental Setup We generate data according to our assumptions by drawing Erdős Rènyi DAGs using $X_j|\mathbf{Pa}_j \sim \mathrm{MLR}\left(\mathbf{B}_j, \boldsymbol{\gamma}^j, \sigma^2\right)$ with Gaussian additive noise $N_j \sim \mathcal{N}(0,1)$ and ensuring that the linear coefficients $\mathbf{B}_j$ are bounded away from zero, $\boldsymbol{\beta}_{jk} \in [-1,-0.25] \cup [0.25,1]$ and similarly from one another. To avoid issues related to Var-sortability and R^2-sortability [Reisach et al., 2021] we generate an internally standardized structural causal model (iSCM) [Ormaniec et al., 2024].

The experiments address the effect of several parameters: the number of observed $N_X \in \{5, \dots 20\}$ and latent variables $N_Z \in \{0, \dots, 10\}$, number of latent classes $K \in \{2, \dots, 5\}$, fraction of observed variables $p_Z \in [0,1]$ affected by mixing, dag density $p_\mathcal{G} \in [0,1]$, sample size $S \in \{200, ...1000\}$ and a parameter controlling the size of the samples in each group $S_Z \in \{2, \dots, 10\}$; for example, for K=2, we uniformly at random draw $\frac{S}{S_Z}$ samples belong class 0, otherwise assign class 1. By default, we show results for $N_X = 10, N_Z = 4, K = 2, p_Z = 0.5, p_\mathcal{G} = 0.4, S = 500, S_Z = 5$. For a detailed description of the data generation setup, see Appendix D.

6.1 Discovering Mixing Structure

We assess the quality of mixing assignments Z_i using the Adjusted Mutual Information (AMI) averaged over the estimated vs. true assignments for each observed node X_j in a simulated graph $\mathcal{G}$, and the mixing structure in $\mathcal{G}^Z$ using F1 scores (binary edge existence $Z_i \to X_j$) and Jaccard indices (set overlap of each Z_i's observed targets). We include simple baselines that apply mixture modeling without causal information for comparison.

In Fig. 4, we observe reliable recovery of mixing assignments (AMI) and their targets (F1, Jacc) for our approach given the true graph (dashed green) and for the full framework (solid green). Applying a clustering baseline such as GMM over all nodes in the graph, as in [Kumar et al., 2024] (blue, ×), is misspecified in case $N_Z > 1$, as per-node assignments are distinct, hence not surprisingly,

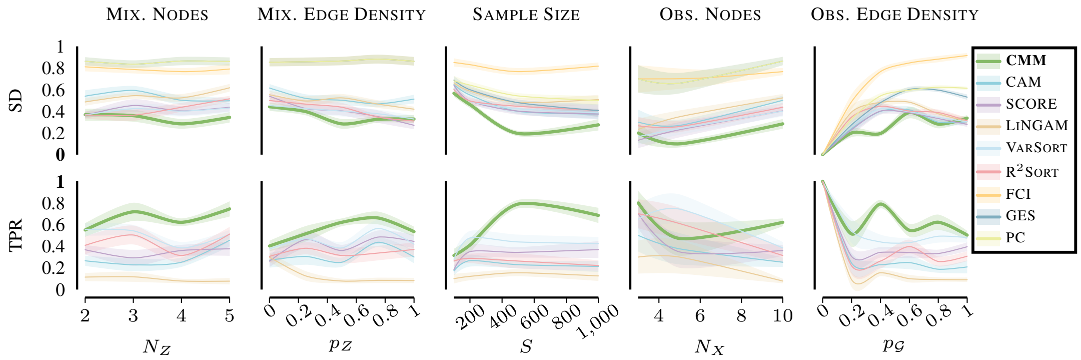

Figure 5: *Discovering Causal Graphs.* In synthetically generated CMMs, we evaluate the quality of the causal DAG over the observed variables in terms of the separation distance (SD) and true positive rate over directed edges (TPR).

performance worsens as N_Z increases (left). Given this, we also apply the models to each node in turn (purple, gray), where gray variants show different instantiation choices. These perform not much better than random splitting in most cases (AMI, F1) and with accurate set recovery (Jacc).

6.2 Discovering Causal Structure

Next, we evaluate the learned causal DAG resp. CPDAG $\mathcal{G}$ against the ground truth $\mathcal{G}^\star$. We consider the separation-based distance metrics proposed by Wahl and Runge, 2024, measuring among others the Separation Distance (SD) over graphs. To demonstrate the strength of our approach in discovering edge orientations in particular, we also compute orientation F1 scores and report true positive rates (TPR). Additional metrics of interest are postponed to the Appendix. Baselines include a range of causal discovery methods, CAM, SCORE, LiNGAM, FCI, GES, PC, VarSort, and R^{2}Sort.

While some baselines perform reasonably well in mixed settings, CMM maintains high accuracy across both structural and causal direction evaluations (Figure 5). We note that Mixture-UTIGSP is not meaningfully applicable here, as there may be multiple mixing variables and no well-defined "observational" part of the dataset as required as input to UTIGSP; thus we will instead consider an experimental setting with a single mixing variable.

Case Study: Mixtures of Interventions Next, we replicate the experimental setup of Kumar et al., 2024 using their data generators to evaluate performance in the mixtures-of-interventions setting. As Figure 6 shows, the GMM used in Mixture-UTIGSP performs well in recovering mixture assignments as expected, given that its modeling assumptions are met in this setting. Our method performs comparably in mixture assignment recovery and recovers the causal graph more reliably (Figure 6 bottom). We also noticed a competitive performance of VarSort in this dataset suggesting potential Var-sortabity which may inflate the performance of the discovery approaches.

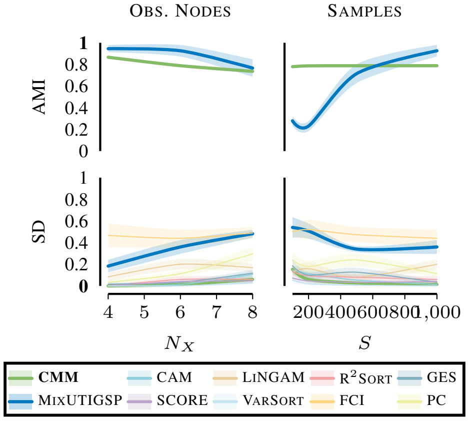

Figure 6: *Mixtures of Interventions.* For data generated from an interventional mixture, we show the quality of mixture separation (AMI, cf. Fig. 4) and causal DAG discovery (SD, cf. Fig. 5).

Case Study: Flow Cytometry Data Finally, we investigate the real-world flow cytometry dataset curated by Sachs et al., 2005. The dataset originates from single-cell protein-signalling samples of the human immune response system, where each of the 11 observed variables corresponds to the activity of one compound of interest: either a protein or a phospholipid. The dataset contains (among others) 5 experimental conditions, in each of which a particular molecular modifier has been applied

	MIXED/IV. SAMPLES (AMI)		
TARGET	CMM*	**CMM**	MIXUTIGSP
Akt	0.02	0.04	0.04
PKC	0.26	0.43	**0.49**
PIP2	0.10	**0.10**	0.03
Mek	0.20	**0.20**	0.14
PIP3	0.00	0.00	0.00

Table 1: *Mixing discovery* as in Fig. 4, for the data by Sachs et al., 2005.

	CAUSAL GRAPH	
METRIC	**CMM**	MIXUTIGSP
TP	5	0
FP	10	2
FN	5	10
SD	**0.25**	0.75
S/C	**0.27**	0.57

Table 2: *Causal discovery* as in Fig. 5, for the data by Sachs et al., 2005.

to the cells, such that the activity of exactly one of the 11 compounds of interest is affected; this results in a known change of the measured activity for the corresponding compound. As in previous analyses [Wang et al., 2017b], we combine the data from all experimental conditions into a larger dataset of size 5846, and do not disclose their origin to the algorithm. Hence, in the pooled data, each variable is affected by a latent one.

For example, considering the node "‘Akt‘", there are two mixture components: one is the experimental condition where the so-called Akt inhibitor was applied, directly inhibiting Akt activation; the other mixture component comprises the remaining samples where Akt is in its baseline condition. In particular, the variables Akt, PKC, PIP2, Mek, and PIP3 were manipulated. We test how well, for each given target node, its intervened subsample can be recovered (AMI). The dataset split found by Mixture-UTIGSP appears to match PKC best, similar for our per-variable splits which match PIP2 and MEC slightly better (Table 1). Still, neither method reaches convincing AMI, consistent with the observations [Kumar et al., 2024; Squires et al., 2020] that the interventional targets are difficult to identify in this dataset. In terms of causal discovery, our approach performs better in terms of separation distances (SD, S/C) albeit discovering a number of spurious (FP) edges (Table 2). All other baselines report similarly high false positive directions (10+ FP) with the exception of PC (2 FP). Additionally, some edge directions in the ground truth such as Raf → Mek are subject to debate. We discover the Mek → Raf direction which has been previously discussed as agreeing better with the given data [Mooij et al., 2016].

In summary, the experiments give empirical support for effectively recovering the mixing structure and the causal structure. In Appendix E, we additionally (i) compare the GES to the TOPIC instantiation; (ii) study the effect of latent mixing variables on causal discovery algorithms; and (iii) compare functional forms both in the data generation as well as during scoring.

7 Conclusion

We address the problem that real-world datasets rarely come from a fixed data-generating process, but could be a combination of subpopulations with distinct causal mechanisms. This gives rise to a causal mixture model in the sense that each effect given its causes results from a finite mixture of linear regressions. We characterize this model in our work and establish theoretical results showing that consistent scoring criteria, such as the latent-aware BIC, allow causal identifiability. Complementary to these insights, we propose a practical implementation for causal discovery using this score which we demonstrate to have strong empirical performance in various settings.

In the real-world case study [Sachs et al., 2005], while the approaches recover the causal graph structure to an extent, we observed limited ability of both the CMM and Mixture-UTIGSP to discover the intervention targets, likely due to the strong assumption of linearity. As our proposed approach can in principle easily incorporate richer models, future work could study scoring criteria and theoretical guarantees for non-linear mixtures, encouraged by a proof-of-concept experiment that we provide in Appendix E. Future work could also study how to further interpret the meaning of a given Z, especially when it points to previously unknown states, for example, by exploring explainability approaches such as LIME [Ribeiro et al., 2016] or Shapley values [Lundberg and Lee, 2017]. Furthermore, invoking Expectation Maximization at every scoring step comes with drawbacks regarding the scalability of our method, especially when relying on random restarts, therefore subsequent analysis could devise algorithmic approaches to reduce this overhead.

Acknowledgements

We would like to thank the anonymous reviewers for their helpful feedback.

References

Judea Pearl (2009). *Causality: Models, Reasoning and Inference*. Cambridge University Press.

Amir Hossein Hasanpour, Mahdi Sepidarkish, Abolfazl Mollalo, Ali Ardekani, Mustafa Almukhtar, Amal Mechaal, Seyed Reza Hosseini, Masoumeh Bayani, Mostafa Javanian, and Ali Rostami (2023). "The global prevalence of methicillin-resistant Staphylococcus aureus colonization in residents of elderly care centers: a systematic review and meta-analysis". In: *Antimicrobial Resistance & Infection Control* 12.1, p. 4.

Tom Li, Mark Walker, and David De Oliveira (Dec. 2022). "Vancomycin Resistance in Enterococcus and Staphylococcus aureus". In: *Microorganisms* 11, p. 24. DOI: 10 . 3390 / microorganisms11010024.

Mathilde Boumasmoud, Vanina Dengler Haunreiter, Tiziano A Schweizer, Lilly Meyer, Bhavya Chakrakodi, Peter W Schreiber, Kati Seidl, Denise Kühnert, Roger D Kouyos, and Annelies S Zinkernagel (2022). "Genomic Surveillance of Vancomycin-Resistant Enterococcus faecium Reveals Spread of a Linear Plasmid Conferring a Nutrient Utilization Advantage". In: *mBio* 13.2, e0377121. ISSN: 2150-7511. DOI: 10.1128/mbio.03771-21.

S. Arredondo-Alonso, J. Top, A. McNally, S. Puranen, M. Pesonen, J. Pensar, P. Marttinen, J. C. Braat, M. R. C. Rogers, W. van Schaik, S. Kaski, R. J. L. Willems, J. Corander, and A. C. Schürch (2020). "Plasmids Shaped the Recent Emergence of the Major Nosocomial Pathogen Enterococcus faecium". In: *mBio* 11.1, 10.1128/mbio.03284–19. DOI: 10.1128/mbio.03284-19.

Yanguang Cong, Sijin Yang, and Xiancai Rao (Oct. 2019). "Vancomycin resistant Staphylococcus aureus infections: A review of case updating and clinical features". In: *Journal of Advanced Research* 21. DOI: 10.1016/j.jare.2019.10.005.

Biwei Huang, Kun Zhang, Jiji Zhang, Joseph Ramsey, Ruben Sanchez-Romero, Clark Glymour, and Bernhard Schölkopf (2020). "Causal Discovery from Heterogeneous/Nonstationary Data". In: 21.1. ISSN: 1532-4435.

Joris M. Mooij, Sara Magliacane, and Tom Claassen (2016). "Joint Causal Inference from Multiple Contexts". In: *J. Mach. Learn. Res.* 21, 99:1–99:108. URL: https://api.semanticscholar.org/CorpusID:126017772.

Chandler Squires, Yuhao Wang, and Caroline Uhler (2020). "Permutation-Based Causal Structure Learning with Unknown Intervention Targets". In: *Proceedings of the 36th Conference on Uncertainty in Artificial Intelligence (UAI)*. Ed. by Jonas Peters and David Sontag. Vol. 124. Proceedings of Machine Learning Research. PMLR, pp. 1039–1048.

Abhinav Kumar, Kirankumar Shiragur, and Caroline Uhler (2024). "Learning Mixtures of Unknown Causal Interventions". In: *The Thirty-eighth Annual Conference on Neural Information Processing Systems*. URL: https://openreview.net/forum?id=aC9mB1PqYJ.

Christian Hennig (July 2000). "Identifiablity of Models for Clusterwise Linear Regression". In: *J. Classification* 17, pp. 273–296. DOI: 10.1007/s003570000022.

Bijan Mazaheri, Spencer Gordon, Yuval Rabani, and Leonard Schulman (Nov. 2023). "Causal Discovery under Latent Class Confounding". In: *arXiv e-prints*, arXiv:2311.07454, arXiv:2311.07454. DOI: 10.48550/arXiv.2311.07454. arXiv: 2311.07454 [cs.LG].

David Maxwell Chickering (2002). "Optimal structure identification with greedy search". In: *Journal of machine learning research* 3.Nov, pp. 507–554.

Sascha Xu, Sarah Mameche, and Jilles Vreeken (2025). "Information-Theoretic Causal Discovery in Topological Order". In: *The 28th International Conference on Artificial Intelligence and Statistics*. URL: https://openreview.net/forum?id=9pjJXQWYXc.

Karen Sachs, Omar Perez, Dana Pe'er, Douglas Lauffenburger, and Garry Nolan (2005). "Causal Protein-Signaling Networks Derived from Multiparameter Single-Cell Data". In: *Science*, pp. 523–9.

C. F. Jeff Wu (1983). "On the Convergence Properties of the EM Algorithm". In: *The Annals of Statistics*, pp. 95–103.

Christopher M. Bishop (2006). *Pattern Recognition and Machine Learning (Information Science and Statistics)*. Berlin, Heidelberg: Springer-Verlag. ISBN: 0387310738.

Shohei Shimizu, Patrik O Hoyer, Aapo Hyvärinen, Antti Kerminen, and Michael Jordan (2006). "A linear non-Gaussian acyclic model for causal discovery." In: *Journal of Machine Learning Research* 7.10.

Sivaraman Balakrishnan, Martin J. Wainwright, and Bin Yu (Feb. 2017). "Statistical Guarantees for the EM Algorithm: From Population to Sample-Based Analysis". In: *The Annals of Statistics*, pp. 77–120.

Nguyen Xuan Vinh, Julien Epps, and James Bailey (2010). "Information Theoretic Measures for Clusterings Comparison: Variants, Properties, Normalization and Correction for Chance". In: *Journal of Machine Learning Research* 11.95, pp. 2837–2854. URL: `http://jmlr.org/papers/v11/vinh10a.html`.

Peter Spirtes, Clark Glymour, and Richard Scheines (2001). *Causation, prediction, and search*. MIT press.

Biwei Huang, Kun Zhang, Yizhu Lin, Bernhard Schölkopf, and Clark Glymour (2018). "Generalized Score Functions for Causal Discovery". In: *Proceedings of the 24th ACM SIGKDD International Conference on Knowledge Discovery and Data Mining*. KDD '18. London, United Kingdom: Association for Computing Machinery, 1551–1560. ISBN: 9781450355520. DOI: `10.1145/3219819.3220104`.

Patrik Hoyer, Dominik Janzing, Joris M Mooij, Jonas Peters, and Bernhard Schölkopf (2008). "Nonlinear causal discovery with additive noise models". In: *Advances in neural information processing systems* 21.

Peter Bühlmann, Jonas Peters, and Jan Ernest (2014). "CAM: Causal additive models, high-dimensional order search and penalized regression". In: *The Annals of Statistics* 42.6, pp. 2526–2556.

Paul Rolland, Volkan Cevher, Matthäus Kleindessner, Chris Russell, Dominik Janzing, Bernhard Schölkopf, and Francesco Locatello (2022). "Score matching enables causal discovery of nonlinear additive noise models". In: *International Conference on Machine Learning*. PMLR, pp. 18741–18753.

Francesco Montagna, Nicoletta Noceti, Lorenzo Rosasco, Kun Zhang, and Francesco Locatello (Aug. 10, 2023). "Scalable Causal Discovery with Score Matching". In: *Proceedings of the Second Conference on Causal Learning and Reasoning*. Conference on Causal Learning and Reasoning. PMLR, pp. 752–771.

Xun Zheng, Bryon Aragam, Pradeep K Ravikumar, and Eric P Xing (2018). "Dags with no tears: Continuous optimization for structure learning". In: *Advances in neural information processing systems* 31.

Alexander G. Reisach, Christof Seiler, and Sebastian Weichwald (Feb. 2021). "Beware of the Simulated DAG! Causal Discovery Benchmarks May Be Easy To Game". In: *arXiv e-prints*, arXiv:2102.13647, arXiv:2102.13647. DOI: `10.48550/arXiv.2102.13647`. arXiv: `2102.13647 [stat.ML]`.

Alexander G. Reisach, Myriam Tami, Christof Seiler, Antoine Chambaz, and Sebastian Weichwald (2023). "A scale-invariant sorting criterion to find a causal order in additive noise models". In: *Proceedings of the 37th International Conference on Neural Information Processing Systems*. NIPS '23. New Orleans, LA, USA: Curran Associates Inc.

Peter Spirtes, Clark Glymour, and Richard Scheines (1993). "Causation, prediction, and search". In: URL: `https://api.semanticscholar.org/CorpusID:117765107`.

B. Schölkopf, F. Locatello, S. Bauer, N. R. Ke, N. Kalchbrenner, A. Goyal, and Y. Bengio (2021). "Toward Causal Representation Learning". In: *Proceedings of the IEEE* 109.5, pp. 612–634. DOI: `10.1109/JPROC.2021.3058954`. URL: `https://ieeexplore.ieee.org/stamp/stamp.jsp?arnumber=9363924`.

Sarah Mameche, David Kaltenpoth, and Jilles Vreeken (2023). "Learning causal models under independent changes". In.

Alain Hauser and Peter Bühlmann (Mar. 2013). "Jointly interventional and observational data: Estimation of interventional Markov equivalence classes of directed acyclic graphs". In: 77. DOI: `10.1111/rssb.12071`.

Yuhao Wang, Liam Solus, Karren Yang, and Caroline Uhler (2017a). "Permutation-based Causal Inference Algorithms with Interventions". In: *Advances in Neural Information Processing Systems*. Ed. by I. Guyon, U. Von Luxburg, S. Bengio, H. Wallach, R. Fergus, S. Vishwanathan, and R. Garnett. Vol. 30. Curran Associates, Inc. URL: `https://proceedings.neurips.cc/paper_files/paper/2017/file/275d7fb2fd45098ad5c3ece2ed4a2824-Paper.pdf`.

Jakob Runge (2020). "Discovering contemporaneous and lagged causal relations in autocorrelated nonlinear time series datasets". In: *Proceedings of the 36th Conference on Uncertainty in Artificial Intelligence (UAI)*. Ed. by Jonas Peters and David Sontag. Vol. 124. Proceedings of Machine Learning Research. PMLR, pp. 1388–1397.

Elena Saggioro, Jana de Wiljes, Marlene Kretschmer, and Jakob Runge (2020). "Reconstructing regime-dependent causal relationships from observational time series". In: *Chaos: An Interdisciplinary Journal of Nonlinear Science*.

Geoffrey J. McLachlan and David Peel (2000). *Finite mixture models*. Vol. 299. Probability and Statistics – Applied Probability and Statistics Section. New York: Wiley.

Shoubo Hu, Zhitang Chen, Vahid Partovi Nia, Laiwan Chan, and Yanhui Geng (2018). "Causal inference and mechanism clustering of a mixture of additive noise models". In: *Proceedings of the 32nd International Conference on Neural Information Processing Systems*. NIPS'18. Montréal, Canada: Curran Associates Inc., 5212–5222.

Kwangho Kim, Jisu Kim, and Edward H. Kennedy (2024). "Causal K-Means Clustering". In: *ArXiv* abs/2405.03083. URL: `https://api.semanticscholar.org/CorpusID:269605158`.

Bijan Mazaheri, Chandler Squires, and Caroline Uhler (2025). "Synthetic Potential Outcomes and Causal Mixture Identifiability". In: *The 28th International Conference on Artificial Intelligence and Statistics*. URL: `https://openreview.net/forum?id=J1CJaSnmKg`.

J. Peters and P. Bühlmann (2013). "Identifiability of Gaussian structural equation models with equal error variances". In: *Biometrika*.

Weronika Ormaniec, Scott Sussex, Lars Lorch, Bernhard Schölkopf, and Andreas Krause (June 2024). "Standardizing Structural Causal Models". In: *arXiv e-prints*, arXiv:2406.11601, arXiv:2406.11601. DOI: `10.48550/arXiv.2406.11601`. arXiv: `2406.11601 [cs.LG]`.

Jonas Wahl and Jakob Runge (Feb. 2024). "Separation-based distance measures for causal graphs". In: *arXiv e-prints*, arXiv:2402.04952, arXiv:2402.04952. DOI: `10.48550/arXiv.2402.04952`. arXiv: `2402.04952 [stat.ME]`.

Yuhao Wang, Liam Solus, Karren Dai Yang, and Caroline Uhler (2017b). "Permutation-based causal inference algorithms with interventions". In: *Proceedings of the 31st International Conference on Neural Information Processing Systems*. NIPS'17. Long Beach, California, USA: Curran Associates Inc., 5824–5833. ISBN: 9781510860964.

Marco Tulio Ribeiro, Sameer Singh, and Carlos Guestrin (2016). ""Why Should I Trust You?": Explaining the Predictions of Any Classifier". In: *Proceedings of the 22nd ACM SIGKDD International Conference on Knowledge Discovery and Data Mining*. Association for Computing Machinery. DOI: `10.1145/2939672.2939778`.

Scott M. Lundberg and Su-In Lee (2017). "A unified approach to interpreting model predictions". In: *Proceedings of the 31st International Conference on Neural Information Processing Systems*.

NeurIPS Paper Checklist

1. **Claims**

   Question: Do the main claims made in the abstract and introduction accurately reflect the paper's contributions and scope?

   Answer: [Yes]

   Justification: The abstract and introduction describe the scope of the problem setting, enumerate contributions, and limitations of the scope (such as linear modelling assumptions).

   Guidelines:

   - The answer NA means that the abstract and introduction do not include the claims made in the paper.
   - The abstract and/or introduction should clearly state the claims made, including the contributions made in the paper and important assumptions and limitations. A No or NA answer to this question will not be perceived well by the reviewers.
   - The claims made should match theoretical and experimental results, and reflect how much the results can be expected to generalize to other settings.
   - It is fine to include aspirational goals as motivation as long as it is clear that these goals are not attained by the paper.

2. **Limitations**

   Question: Does the paper discuss the limitations of the work performed by the authors?

   Answer: [Yes]

   Justification: Modeling assumptions and limitations are stated. The conclusion includes limitations with future work options. Empirical limitations are explored in the experimental evaluation which, while depending on assumptions (functional model stated in the experimental setup), evaluates a wide range of parameters and baselines, and also tests data generators not created by the authors (mixture of interventions) and on a real-world dataset.

   Guidelines:

   - The answer NA means that the paper has no limitation while the answer No means that the paper has limitations, but those are not discussed in the paper.
   - The authors are encouraged to create a separate "Limitations" section in their paper.
   - The paper should point out any strong assumptions and how robust the results are to violations of these assumptions (e.g., independence assumptions, noiseless settings, model well-specification, asymptotic approximations only holding locally). The authors should reflect on how these assumptions might be violated in practice and what the implications would be.
   - The authors should reflect on the scope of the claims made, e.g., if the approach was only tested on a few datasets or with a few runs. In general, empirical results often depend on implicit assumptions, which should be articulated.
   - The authors should reflect on the factors that influence the performance of the approach. For example, a facial recognition algorithm may perform poorly when image resolution is low or images are taken in low lighting. Or a speech-to-text system might not be used reliably to provide closed captions for online lectures because it fails to handle technical jargon.
   - The authors should discuss the computational efficiency of the proposed algorithms and how they scale with dataset size.
   - If applicable, the authors should discuss possible limitations of their approach to address problems of privacy and fairness.
   - While the authors might fear that complete honesty about limitations might be used by reviewers as grounds for rejection, a worse outcome might be that reviewers discover limitations that aren't acknowledged in the paper. The authors should use their best judgment and recognize that individual actions in favor of transparency play an important role in developing norms that preserve the integrity of the community. Reviewers will be specifically instructed to not penalize honesty concerning limitations.

3. **Theory assumptions and proofs**

   Question: For each theoretical result, does the paper provide the full set of assumptions and a complete (and correct) proof?

   Answer: [Yes]

   Justification: Theoretical statements are proven and all relevant assumptions listed.

   Guidelines:

- The answer NA means that the paper does not include theoretical results.
- All the theorems, formulas, and proofs in the paper should be numbered and cross-referenced.
- All assumptions should be clearly stated or referenced in the statement of any theorems.
- The proofs can either appear in the main paper or the supplemental material, but if they appear in the supplemental material, the authors are encouraged to provide a short proof sketch to provide intuition.
- Inversely, any informal proof provided in the core of the paper should be complemented by formal proofs provided in appendix or supplemental material.
- Theorems and Lemmas that the proof relies upon should be properly referenced.

4. **Experimental result reproducibility**

   Question: Does the paper fully disclose all the information needed to reproduce the main experimental results of the paper to the extent that it affects the main claims and/or conclusions of the paper (regardless of whether the code and data are provided or not)?

   Answer: [Yes]

   Justification: The code for running the proposed algorithm, the baselines shown, as well as for reproducing all experiments shown in the evaluation will be included in the supplementary material, with reasonable guidelines (scripts for reproducing the data used in each Figure).

   Guidelines:

   - The answer NA means that the paper does not include experiments.
   - If the paper includes experiments, a No answer to this question will not be perceived well by the reviewers: Making the paper reproducible is important, regardless of whether the code and data are provided or not.
   - If the contribution is a dataset and/or model, the authors should describe the steps taken to make their results reproducible or verifiable.
   - Depending on the contribution, reproducibility can be accomplished in various ways. For example, if the contribution is a novel architecture, describing the architecture fully might suffice, or if the contribution is a specific model and empirical evaluation, it may be necessary to either make it possible for others to replicate the model with the same dataset, or provide access to the model. In general. releasing code and data is often one good way to accomplish this, but reproducibility can also be provided via detailed instructions for how to replicate the results, access to a hosted model (e.g., in the case of a large language model), releasing of a model checkpoint, or other means that are appropriate to the research performed.
   - While NeurIPS does not require releasing code, the conference does require all submissions to provide some reasonable avenue for reproducibility, which may depend on the nature of the contribution. For example
     (a) If the contribution is primarily a new algorithm, the paper should make it clear how to reproduce that algorithm.
     (b) If the contribution is primarily a new model architecture, the paper should describe the architecture clearly and fully.
     (c) If the contribution is a new model (e.g., a large language model), then there should either be a way to access this model for reproducing the results or a way to reproduce the model (e.g., with an open-source dataset or instructions for how to construct the dataset).
     (d) We recognize that reproducibility may be tricky in some cases, in which case authors are welcome to describe the particular way they provide for reproducibility. In the case of closed-source models, it may be that access to the model is limited in some way (e.g., to registered users), but it should be possible for other researchers to have some path to reproducing or verifying the results.

5. **Open access to data and code**

   Question: Does the paper provide open access to the data and code, with sufficient instructions to faithfully reproduce the main experimental results, as described in supplemental material?

   Answer: [Yes]

   Justification: Code and data can be released alongside the manuscript and to the best of our efforts contain all necessary scripts and environments for reproducing the results.

   Guidelines:

- The answer NA means that paper does not include experiments requiring code.
- Please see the NeurIPS code and data submission guidelines (`https://nips.cc/public/guides/CodeSubmissionPolicy`) for more details.
- While we encourage the release of code and data, we understand that this might not be possible, so "No" is an acceptable answer. Papers cannot be rejected simply for not including code, unless this is central to the contribution (e.g., for a new open-source benchmark).
- The instructions should contain the exact command and environment needed to run to reproduce the results. See the NeurIPS code and data submission guidelines (`https://nips.cc/public/guides/CodeSubmissionPolicy`) for more details.
- The authors should provide instructions on data access and preparation, including how to access the raw data, preprocessed data, intermediate data, and generated data, etc.
- The authors should provide scripts to reproduce all experimental results for the new proposed method and baselines. If only a subset of experiments are reproducible, they should state which ones are omitted from the script and why.
- At submission time, to preserve anonymity, the authors should release anonymized versions (if applicable).
- Providing as much information as possible in supplemental material (appended to the paper) is recommended, but including URLs to data and code is permitted.

6. **Experimental setting/details**

   Question: Does the paper specify all the training and test details (e.g., data splits, hyperparameters, how they were chosen, type of optimizer, etc.) necessary to understand the results?

   Answer: [Yes]

   Justification: Details necessary to understand the results are to the best of our efforts included in the evaluation section, such as the considered experimental parameters, and the baselines were run without modifying the standard hyperparameters in their off the shelf implementations.

   Guidelines:
   - The answer NA means that the paper does not include experiments.
   - The experimental setting should be presented in the core of the paper to a level of detail that is necessary to appreciate the results and make sense of them.
   - The full details can be provided either with the code, in appendix, or as supplemental material.

7. **Experiment statistical significance**

   Question: Does the paper report error bars suitably and correctly defined or other appropriate information about the statistical significance of the experiments?

   Answer: [Yes]

   Justification: The main plots show error regions for the methods to account for randomness in the synthetic data generation.

   Guidelines:
   - The answer NA means that the paper does not include experiments.
   - The authors should answer "Yes" if the results are accompanied by error bars, confidence intervals, or statistical significance tests, at least for the experiments that support the main claims of the paper.
   - The factors of variability that the error bars are capturing should be clearly stated (for example, train/test split, initialization, random drawing of some parameter, or overall run with given experimental conditions).
   - The method for calculating the error bars should be explained (closed form formula, call to a library function, bootstrap, etc.)
   - The assumptions made should be given (e.g., Normally distributed errors).
   - It should be clear whether the error bar is the standard deviation or the standard error of the mean.
   - It is OK to report 1-sigma error bars, but one should state it. The authors should preferably report a 2-sigma error bar than state that they have a 96% CI, if the hypothesis of Normality of errors is not verified.
   - For asymmetric distributions, the authors should be careful not to show in tables or figures symmetric error bars that would yield results that are out of range (e.g. negative error rates).

- If error bars are reported in tables or plots, The authors should explain in the text how they were calculated and reference the corresponding figures or tables in the text.

8. **Experiments compute resources**

   Question: For each experiment, does the paper provide sufficient information on the computer resources (type of compute workers, memory, time of execution) needed to reproduce the experiments?

   Answer: [Yes]

   Justification: All experiments can be reproduced with standard commodity hardware.

   Guidelines:

   - The answer NA means that the paper does not include experiments.
   - The paper should indicate the type of compute workers CPU or GPU, internal cluster, or cloud provider, including relevant memory and storage.
   - The paper should provide the amount of compute required for each of the individual experimental runs as well as estimate the total compute.
   - The paper should disclose whether the full research project required more compute than the experiments reported in the paper (e.g., preliminary or failed experiments that didn't make it into the paper).

9. **Code of ethics**

   Question: Does the research conducted in the paper conform, in every respect, with the NeurIPS Code of Ethics `https://neurips.cc/public/EthicsGuidelines`?

   Answer: [Yes]

   Justification: There are no ethical considerations with e.g. experiments and research methods and to our knowledge no major ethical concerns with the approach.

   Guidelines:

   - The answer NA means that the authors have not reviewed the NeurIPS Code of Ethics.
   - If the authors answer No, they should explain the special circumstances that require a deviation from the Code of Ethics.
   - The authors should make sure to preserve anonymity (e.g., if there is a special consideration due to laws or regulations in their jurisdiction).

10. **Broader impacts**

    Question: Does the paper discuss both potential positive societal impacts and negative societal impacts of the work performed?

    Answer: [NA]

    Justification: There are no direct negative societal impact of this research in our view as this work is part of foundational research. Its practical applicability is towards gaining causal insights in the sciences and is mostly unrelated to the malicious and unintended uses mentioned in the guidelines.

    Guidelines:

    - The answer NA means that there is no societal impact of the work performed.
    - If the authors answer NA or No, they should explain why their work has no societal impact or why the paper does not address societal impact.
    - Examples of negative societal impacts include potential malicious or unintended uses (e.g., disinformation, generating fake profiles, surveillance), fairness considerations (e.g., deployment of technologies that could make decisions that unfairly impact specific groups), privacy considerations, and security considerations.
    - The conference expects that many papers will be foundational research and not tied to particular applications, let alone deployments. However, if there is a direct path to any negative applications, the authors should point it out. For example, it is legitimate to point out that an improvement in the quality of generative models could be used to generate deepfakes for disinformation. On the other hand, it is not needed to point out that a generic algorithm for optimizing neural networks could enable people to train models that generate Deepfakes faster.
    - The authors should consider possible harms that could arise when the technology is being used as intended and functioning correctly, harms that could arise when the technology is being used as intended but gives incorrect results, and harms following from (intentional or unintentional) misuse of the technology.
    - If there are negative societal impacts, the authors could also discuss possible mitigation strategies (e.g., gated release of models, providing defenses in addition to attacks,

mechanisms for monitoring misuse, mechanisms to monitor how a system learns from feedback over time, improving the efficiency and accessibility of ML).

11. **Safeguards**

    Question: Does the paper describe safeguards that have been put in place for responsible release of data or models that have a high risk for misuse (e.g., pretrained language models, image generators, or scraped datasets)?

    Answer: [NA]

    Justification: The paper poses no such risks.

    Guidelines:
    - The answer NA means that the paper poses no such risks.
    - Released models that have a high risk for misuse or dual-use should be released with necessary safeguards to allow for controlled use of the model, for example by requiring that users adhere to usage guidelines or restrictions to access the model or implementing safety filters.
    - Datasets that have been scraped from the Internet could pose safety risks. The authors should describe how they avoided releasing unsafe images.
    - We recognize that providing effective safeguards is challenging, and many papers do not require this, but we encourage authors to take this into account and make a best faith effort.

12. **Licenses for existing assets**

    Question: Are the creators or original owners of assets (e.g., code, data, models), used in the paper, properly credited and are the license and terms of use explicitly mentioned and properly respected?

    Answer: [Yes]

    Justification: The widely used dataset by Sachs et al. (2005) was considered which is cited. Code for reproducing various causal discovery baselines is available under public licenses and the corresponding works have been cited.

    Guidelines:
    - The answer NA means that the paper does not use existing assets.
    - The authors should cite the original paper that produced the code package or dataset.
    - The authors should state which version of the asset is used and, if possible, include a URL.
    - The name of the license (e.g., CC-BY 4.0) should be included for each asset.
    - For scraped data from a particular source (e.g., website), the copyright and terms of service of that source should be provided.
    - If assets are released, the license, copyright information, and terms of use in the package should be provided. For popular datasets, `paperswithcode.com/datasets` has curated licenses for some datasets. Their licensing guide can help determine the license of a dataset.
    - For existing datasets that are re-packaged, both the original license and the license of the derived asset (if it has changed) should be provided.
    - If this information is not available online, the authors are encouraged to reach out to the asset's creators.

13. **New assets**

    Question: Are new assets introduced in the paper well documented and is the documentation provided alongside the assets?

    Answer: [NA]

    Justification: the paper does not release new assets.

    Guidelines:
    - The answer NA means that the paper does not release new assets.
    - Researchers should communicate the details of the dataset/code/model as part of their submissions via structured templates. This includes details about training, license, limitations, etc.
    - The paper should discuss whether and how consent was obtained from people whose asset is used.
    - At submission time, remember to anonymize your assets (if applicable). You can either create an anonymized URL or include an anonymized zip file.

14. **Crowdsourcing and research with human subjects**

Question: For crowdsourcing experiments and research with human subjects, does the paper include the full text of instructions given to participants and screenshots, if applicable, as well as details about compensation (if any)?

Answer: [NA]

Justification: The paper does not involve crowdsourcing nor research with human subjects.

Guidelines:

- The answer NA means that the paper does not involve crowdsourcing nor research with human subjects.
- Including this information in the supplemental material is fine, but if the main contribution of the paper involves human subjects, then as much detail as possible should be included in the main paper.
- According to the NeurIPS Code of Ethics, workers involved in data collection, curation, or other labor should be paid at least the minimum wage in the country of the data collector.

15. **Institutional review board (IRB) approvals or equivalent for research with human subjects**

Question: Does the paper describe potential risks incurred by study participants, whether such risks were disclosed to the subjects, and whether Institutional Review Board (IRB) approvals (or an equivalent approval/review based on the requirements of your country or institution) were obtained?

Answer: [NA]

Justification: The paper does not involve crowdsourcing nor research with human subjects.

Guidelines:

- The answer NA means that the paper does not involve crowdsourcing nor research with human subjects.
- Depending on the country in which research is conducted, IRB approval (or equivalent) may be required for any human subjects research. If you obtained IRB approval, you should clearly state this in the paper.
- We recognize that the procedures for this may vary significantly between institutions and locations, and we expect authors to adhere to the NeurIPS Code of Ethics and the guidelines for their institution.
- For initial submissions, do not include any information that would break anonymity (if applicable), such as the institution conducting the review.

16. **Declaration of LLM usage**

Question: Does the paper describe the usage of LLMs if it is an important, original, or non-standard component of the core methods in this research? Note that if the LLM is used only for writing, editing, or formatting purposes and does not impact the core methodology, scientific rigorousness, or originality of the research, declaration is not required.

Answer: [NA]

Justification: The core ideation, development and presentation of the research does not involve LLMs.

Guidelines:

- The answer NA means that the core method development in this research does not involve LLMs as any important, original, or non-standard components.
- Please refer to our LLM policy (`https://neurips.cc/Conferences/2025/LLM`) for what should or should not be described.

A Preliminaries

In this section, we provide a brief overview of helpful preliminary concepts that, although relevant to our analysis, we assume to be widely familiar in the main target audience of our work; for brevity and clarity, we therefore chose to postpone them away from the main manuscript and into this appendix.

A.1 Structural Causal Models

Given random variables $\boldsymbol{X} = \{X_1, \dots, X_n\}$ we can encode the underlying data generating process (DGP) as a structural equation model (SEM) [Koller and Friedman, 2009]; this model encodes a set of hypotheses on this process in the form of one functional dependency f_j for each random variable $X_j \in \boldsymbol{X}$, so that

$$X_j = f_j(\boldsymbol{X}_j) \qquad \text{with } \boldsymbol{X}_j \subseteq \boldsymbol{X} \setminus \{X_j\}\,. \tag{10}$$

Of special interest is a structural causal model (SCM) [Bollen, 1989], which is a particular kind of an SEM with additional assumptions that allow it to also model the causal mechanisms of the DGP. Here, the set of random variables $\boldsymbol{X}$ is extended to also include random unobserved variables $\mathbf{U} = \{U_1, \dots, U_n\}$, which play the role of noise. Hence, each functional dependency takes the form

$$X_j = f_j(\boldsymbol{X}_j, U_j) \qquad \text{with } \boldsymbol{X}_j \subseteq \boldsymbol{X} \setminus \{X_j\} \text{ and } U_j \in \mathbf{U}\,. \tag{11}$$

To further study SCMs, we need to establish their correspondence with causal graphs [Pearl, 2009].

A.2 Causal Graphs

Consider a set of random variables $\boldsymbol{X} = \{X_1, \dots, X_n\}$ that follow a distribution $\mathcal{L}_{\boldsymbol{X}}$ that has a joint probability density $p_{\boldsymbol{X}}$ with respect to some appropriate measure, and an (arbitrary) total ordering $X_1 < X_2 < \cdots < X_n$. Then the joint probability density factorises as

$$p_{\boldsymbol{X}}(\mathbf{x}) = \prod_{X_j \in \boldsymbol{X}} p_{X_j|\mathbf{Y}_j}(x, \mathbf{y}_j)\,, \qquad \text{where } \mathbf{Y}_j \subseteq \{X_1, \dots, X_j\} \tag{12}$$

and $\mathbf{y}_j$ are those values out of $\mathbf{x}$ corresponding to the same indices as $\mathbf{Y}_j$. This comes as a direct result of the chain rule and the conditional independence rules. Any such factorisation can be represented as a (fully) directed acyclic graph (DAG) $\mathcal{G} = (\boldsymbol{X}, E)$ with nodes the random variables $\boldsymbol{X}$ and edges the set $E = \cup_{j=1}^{n} \{i \to j | X_i \in \mathbf{Y}_j\}$. In other words, in this graph we add an edge to the dependent variable X_j from each variable in the corresponding conditioning set $\mathbf{Y}_j$ that appears in each factor $p_{X_j|\mathbf{Y}_j}$ of Eq. (12). We further make this relation explicit, by instead writing $\mathbf{Pa}_j = \mathbf{Y}_j$ to indicate that the conditioning set $\mathbf{Y}_j$ serves as the set of direct parents of node X_j in $\mathcal{G}$. Such a graph is called a *Bayesian network* [Koller and Friedman, 2009] and allows for a visual representation of all those independencies that are implied solely from this factorisation of the joint density and irrespective of the form of each factor.

These independencies can be read from the graph in terms of the d-separation [Pearl, 2009].

Definition A.1 (d-separation)**.** For any pairwise disjoint subsets $\mathbf{U}, \mathbf{V}, \mathbf{W} \subseteq \boldsymbol{X}$, and $\mathbf{U}, \mathbf{V} \neq \emptyset$, it is

$$\mathbf{U} \perp\!\!\!\perp \mathbf{V} | \mathbf{W} \iff \text{all paths from any variable in } U \text{ to any of } V \text{ are blocked by } W\,. \tag{13}$$

We call a path blocked if it either

- traverses a section $\to V \to$, $\leftarrow V \leftarrow$ or $\leftarrow V \to$ for some variable $V \in W$, or
- traverses a section $\to V \leftarrow$ where neither V nor any of its descendants are contained in W.

Hence, a Bayesian network $\mathcal{G}$ can be seen as a description of an entire family of distributions that fulfill a given set of conditional independencies. When a distribution $\mathcal{L}_{\boldsymbol{X}}$ exhibits all the conditional independencies that one can read from the graph $\mathcal{G}$, we call $\mathcal{G}$ an I-map of $\mathcal{L}_{\boldsymbol{X}}$ and write $\mathcal{L}_{\boldsymbol{X}} \in I_{\mathcal{G}}$.

In other words, the I-map defines an equivalence relation among all DAGs via the relation $\mathcal{G} \equiv_M \mathcal{G}' \iff I_{\mathcal{G}} = I_{\mathcal{G}'}$, of which each equivalence class is called the *Markov equivalence class* (MEC). When, in addition, each of the factors in the factorisation of Eq. (12) correspond to a functional dependency of an SCM, we call the resulting DAG causal.

A graphical representation of MECs can be given through the common notion of *completed partially directed acyclic graphs* (CPDAGs) [Chickering, 2002] also known under other names such as maximally oriented graphs [Meek, 1997]. A partially directed graph (PDAG) $\mathcal{P}$ contains both undirected and directed edeges, and can be associated to an equivalence class $\mathcal{M}(\mathcal{P})$ with $\mathcal{G} \in \mathcal{M}(\mathcal{P})$ if and only if $\mathcal{G}, \mathcal{P}$ have the same skeleton and v-structures. The notion of completion of PDAGs allows for representing equivalence classes uniquely. To this end, for a given equivalence class $\mathcal{M}$ one distinguishes between *compelled* edges with the same directionality in every member of $\mathcal{M}$, and *reversible* edges otherwise. The completed PDAG $\mathcal{P}$ for $\mathcal{M}$ is then the one having a directed edge for every compelled edge in $\mathcal{M}$, and an undirected edge for every reversible edge in $\mathcal{M}$.

A.3 SCMs and causal graphs

We now return to the assumptions implicit in an SCM.

Assumption 2 (Causal Interpretation)**.** Each functional dependency f_j corresponds to a true causal mechanism in the data, with $\boldsymbol{X}_j$ being the direct causes of the direct effect X_j.

As a corollary, the corresponding causal graph can have no recurrence.

Assumption 3 (Orientation and Acyclicity)**.** The causal graph of an SCM is a DAG.

Hence, we can once again identify the direct causes of each effect X_j with its parents in the corresponding DAG, $\boldsymbol{X}_j = \mathbf{Pa}_j$.

Assumption 4 (Exogeneity of Noise)**.** The random variables $\mathbf{U}$ are exogenous; that is, there are no edges $X_j \to U_i$, for any X_j and any U_i.

Assumption 5 (Independence of Noise)**.** The random variables $\mathbf{U}$ are mutually independent.

In our work, in particular, we consider that part of the noise for each effect X_j is the latent variable La_j, in addition to the typical U_j. Hence, even though for the set $\mathbf{U}$ we do make Assumption 5, we note that this fails to hold for the entire set of exogenous noise sources, which, in our case, is further extended to include all $\boldsymbol{Z}$. As a result, to be more rigorous, we make claims to find the CPDAG corresponding to the conditional distribution $\mathcal{L}_{\boldsymbol{X}|\boldsymbol{Z}}$, rather than the marginal $\mathcal{L}_{\boldsymbol{X}}$.

We remark that, if one is interested in the entire marginal $\mathcal{L}_{\boldsymbol{X}}$, this can be achieved as a two-level algorithm, in which we first use our presented method to infer the Markov equivalence class of $\mathcal{L}_{\boldsymbol{X}|\boldsymbol{Z}}$, and then use the inferred values of each La_j to identify which variables correspond to the same underlying latent Z_i, and finally performing causal structure inference over the values of $\boldsymbol{Z}$ to complete the Markov equivalence class of $\mathcal{L}_{\boldsymbol{X}}$.

In the scope of our work, we hence focus on the conditional $\mathcal{L}_{\boldsymbol{X}|\boldsymbol{Z}}$. In the following section we formally show that we can recover the corresponding underlying Markov equivalence class, as represented by a CPDAG $\mathcal{G}$. Specifically, we next move to formally showing our main claims in Corollary 3.4 on using the proposed latent-aware BIC as a consistent scoring criterion for this purpose.

B Proof of Theorem 3.3

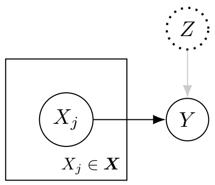

$$\boldsymbol{X} \in \mathbb{R}^n, \ Z \in \mathbb{N}$$
$$Y|\boldsymbol{X} \sim \mathrm{MLR}(\boldsymbol{\theta}),$$
$$\boldsymbol{\theta} = (\mathbf{B}, \boldsymbol{\gamma}, \sigma^2) \in \bigcup_{K \geq 2} \Theta_K$$
$$\Theta_K = (\mathbb{R}^n)^K \times \mathcal{S}^{K-1} \times \mathbb{R}_+$$

Figure B.1: The parameters of the MLR distribution.

In this section we elaborate on the theoretical justification of our method. For this, we make use of the relaxed space constraints to break down our analysis in finer steps. We first show that under mild conditions, the MLR distribution does not degenerate to a Gaussian.

We hence treat the parameters $\boldsymbol{\theta}$ as random variables and assume each MLR distribution in the data generating process to be drawn as follows. First, a finite number $K \geq 2$ of components is arbitrarily fixed; then the tuple $\boldsymbol{\theta} = (\mathbf{B}, \boldsymbol{\gamma}, \sigma^2) \in \Theta_K$ is drawn, where $\Theta_K = (\mathbb{R}^n)^K \times \mathcal{S}^{K-1} \times \mathbb{R}_+$ is the parameter space of the model with K components and $\mathcal{S}^K$ the K-dimensional probability simplex.
Out of this tuple, the linear coefficients are assumed to be drawn from a prior $\mathbf{B} \sim \mu_{\mathbf{B}}^K$, the mixture coefficients from $\boldsymbol{\gamma} \sim \mu_{\boldsymbol{\gamma}}^K$, and a positive variance $\sigma^2 > 0$ from an arbitrary distribution.
Also let $\lambda_{\mathbf{B}}^K$ be the push-forward of the Lebesgue measure on $\mathbb{R}^{n \times K}$ through the homeomorphism of that space with $(\mathbb{R}^n)^K$ and $\lambda_{\boldsymbol{\gamma}}^K$ the Lebesgue measure on $\mathcal{S}^{K-1}$.

Lemma B.1 (Non Gaussianity of Direct Effect). *Let $\boldsymbol{X} \in \mathbb{R}^d$, $Y \in \mathbb{R}$ be random variables such that $Y|\boldsymbol{X} \sim \mathrm{MLR}\left(\mathbf{B}, \boldsymbol{\gamma}, \sigma^2\right)$, with parameters $\boldsymbol{\theta} = (\mathbf{B}, \boldsymbol{\gamma}, \sigma^2) \in \Theta = \cup_{K \geq 2} \Theta_K$. Let the parameter prior μ_Θ be σ-additive; let for each Θ_K the marginal priors of the linear coefficients and the mixture coefficients*[1] *be absolutely continuous with respect to the corresponding Lebesgue measure, that is, $\mu_{\mathbf{B}}^K \ll \lambda_{\mathbf{B}}^K$ and $\mu_{\boldsymbol{\gamma}}^K \ll \lambda_{\boldsymbol{\gamma}}^K$.*
Then the distribution of $Y|\boldsymbol{X}$ is almost surely not a Gaussian.

Proof. Fix a $K \geq 2$. We first show that the MLR distribution with density

$$p_{Y|\mathbf{X}}^{\mathrm{MLR}}(y, \mathbf{x}; \mathbf{B}, \boldsymbol{\gamma}, \sigma^2) = \sum_{k=1}^{K} \gamma_k p_X^{\mathcal{N}}(x; {\boldsymbol{\beta}_k}^\top \mathbf{y}, \sigma^2) \tag{14}$$

almost never degenerates into a Gaussian.

The alternative can only happen under either of the following two conditions:

1. there is only one (active) component in the mixture, or
2. each active component has the same linear coefficients.

For the former condition to hold, it must be that for the drawn $\boldsymbol{\gamma}$ it is $\gamma_k = 1$ for some $1 \leq k \leq K$. The probability of drawing such a $\boldsymbol{\gamma}$ is equal to $\mu_{\boldsymbol{\gamma}}^K(E_K)$ where

$$E_K = \{\boldsymbol{\gamma} \in \mathcal{S}^{K-1} \mid \exists k,\, 1 \leq i \leq K,\, \gamma_k = 1\} \tag{15}$$

is the set of the K extremal points of $\mathcal{S}^{K-1}$. However, E_K is a finite subset of $\mathcal{S}^{K-1}$, and so $\lambda_{\boldsymbol{\gamma}}^K(E_K) = 0$; this, implies that $\mu_{\boldsymbol{\gamma}}^K(E_K) = 0$, since $\mu_{\boldsymbol{\gamma}}^K \ll \lambda_{\boldsymbol{\gamma}}^K$.

To study the latter condition, we treat the domain of the linear coefficients as $\mathbf{B} \in \mathbb{R}^{n \times K}$, which is homeomorphic to $(\mathbb{R}^n)^K$. Denote V_K the set of matrices with all columns equal. This set forms a linear subspace $V_K \subseteq \mathbb{R}^{n \times K}$, as it contains the zero matrix and is closed under scalar multiplication and addition. Additionally, this linear subspace V_K is a proper subspace of $\mathbb{R}^{n \times K}$, as the latter contains matrices with unequal columns, which are not part of V_K. Therefore, the Lebesgue measure of this subspace vanishes, $\lambda_{\mathbf{B}}^K(V_K) = 0$, which in turn implies that $\mu_{\mathbf{B}}^K(V_K) = 0$, due to $\mu_{\mathbf{B}}^K \ll \lambda_{\mathbf{B}}^K$.

We now consider the pre-images $\bar{V}_K = \pi_{\mathbf{B}|K}^{-1}(V_K)$ and $\bar{E}_K = \pi_{\boldsymbol{\gamma}|K}^{-1}(E_K)$ of these sets, where $\pi_{\mathbf{B}|K} : \Theta_K \to \mathbb{R}^{n \times K}$ and $\pi_{\boldsymbol{\gamma}|K} : \Theta_K \to \mathcal{S}^{K-1}$ are the Cartesian projections from the space of parameter tuples in Θ_K to that of the space of linear coefficients and mixing coefficients, respectively. Further, since $\Theta = \bigcup_{K \geq 2} \Theta_K$, it is also that $\bar{V}_K, \bar{E}_K \in \Theta$. However, since the measure of both V_K and E_K vanished in the corresponding marginal measures, $\mu_{\mathbf{B}}^K, \mu_{\boldsymbol{\gamma}}^K$, respectively, it must also be that $\mu_\Theta(\bar{V}_K) = \mu_\Theta(\bar{E}_K) = 0$.

Hence, the probability that for a given K the distribution degenerates is equal to $\mu_\Theta(\bar{D}_K)$, which we define as $\bar{D}_K \coloneqq \bar{V}_K \cup \bar{E}_K$. Now, by the union bound $\mu_\Theta(\bar{D}_K) \leq \mu_\Theta(\bar{V}_K) + \mu_\Theta(\bar{E}_K) = 0$.

Finally, we can bound the probability that the MLR distribution degenerates into a Gaussian for an arbitrarily drawn number of components. Let $\bar{D} \subseteq \Theta$ be the parameters of the MLR distribution that correspond to the cases that degenerate into a Gaussian, for which it is $\bar{D} = \bigcup_{K \geq 2} \bar{D}_K$. By the σ-additivity of μ_Θ we get

$$\mathbb{P}\big(\{\mathrm{MLR}\ \textit{degenerates into Gaussian}\}\big) = \mu_\Theta(\bar{D}) = \mu_\Theta\big(\bigcup_{K \geq 2} \bar{D}_K\big) = \sum_{K \geq 2} \mu_\Theta(\bar{D}_K) = 0\,, \tag{16}$$

which concludes the proof. □

To show identifiability, we need to be able to distinguish, under the true hypothesis $Y|\boldsymbol{X} \sim \mathrm{MLR}$, between all competing hypotheses of Fig. B.2.

Theorem 3.3 (Local Consistency of $\mathrm{BIC}_{\hat{Z}}^{\mathrm{ML}}$). *Let $\mathcal{D} = \{\mathbf{x}_1, \ldots, \mathbf{x}_r\}$ be observations of random variables $\boldsymbol{X}$, Y, such that $\boldsymbol{X}|Y \sim \mathrm{MLR}\left(\mathbf{B}, \boldsymbol{\gamma}, \sigma^2\right)$, with general parameters $\boldsymbol{\theta}$ (see Lemma B.1). Then, out of the structural hypotheses depicted in Fig. 3 the $\mathrm{BIC}_{\hat{Z}}^{ML}$ score of the ground truth hypothesis $\mathcal{G}_{cs}^h$ is asymptotically larger than any of the alternative ones, $\mathcal{G}_{ws}^h$ and $\mathcal{G}_{me}^h$, almost surely.*

[1] Note that a weaker condition is needed for the mixture coefficients, namely that at least two components have positive probability. This more general requirement, however, is already general enough and easier to treat.

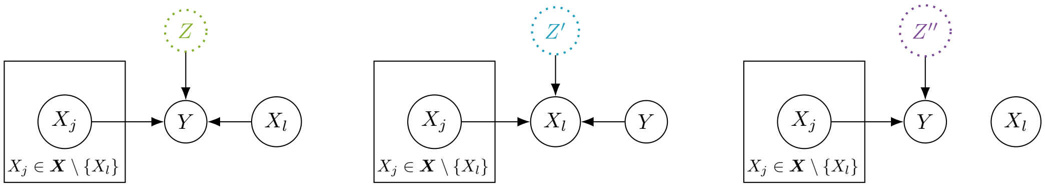
Z
X_j
Y
X_l
$X_j \in \boldsymbol{X} \setminus \{X_l\}$
Z'
X_j
X_l
Y
$X_j \in \boldsymbol{X} \setminus \{X_l\}$
Z''
X_j
Y
X_l
$X_j \in \boldsymbol{X} \setminus \{X_l\}$

(a) Correct Structure $\mathcal{G}^{\mathrm{h}}_{\mathrm{cs}}$ (b) Wrong Sink $\mathcal{G}^{\mathrm{h}}_{\mathrm{ws}}$ (c) Missing edge $\mathcal{G}^{\mathrm{h}}_{\mathrm{me}}$

Figure B.2: *Identifiable Cases.* Under mild assumptions, when Z has at least two mixing components, all of the shown DAGs are identifiable.

Proof. This claim builds on the established properties of the vanilla BIC score. Here, we treat $\boldsymbol{X} \setminus \{X_l\}$ as nuisance parameters, and we focus on single edge modifications, between the sink of each structural hypothesis and the node on the right of each depiction.

We first consider the pair $\mathcal{G}^{\mathrm{h}}_{\mathrm{cs}}$ and $\mathcal{G}^{\mathrm{h}}_{\mathrm{ws}}$. In this case, since the $\mathrm{BIC}^{\mathrm{ML}}_{\hat{Z}}$ is based on the Maximum Likelihood Estimate (MLE) estimates $\hat{\boldsymbol{\theta}}$ of the true parameter values $\boldsymbol{\theta}$, and the MLE estimate is asymptotically unbiased, then the the correct model $\mathcal{G}^{\mathrm{h}}_{\mathrm{cs}}$ and the one arising from the alternate hypothesis $\mathcal{G}^{\mathrm{h}}_{\mathrm{ws}}$ have the same number of parameters, while at the same time the likelihood under $\mathcal{G}^{\mathrm{h}}_{\mathrm{cs}}$ is larger than that of $\mathcal{G}^{\mathrm{h}}_{\mathrm{ws}}$. Hence, in this case the $\mathrm{BIC}^{\mathrm{ML}}_{\hat{Z}}$ value is an increasing function of only the likelihood, and hence it must be that also $\mathrm{BIC}^{\mathrm{ML}}_{\hat{Z}}(\mathcal{G}^{\mathrm{h}}_{\mathrm{cs}}) > \mathrm{BIC}^{\mathrm{ML}}_{\hat{Z}}(\mathcal{G}^{\mathrm{h}}_{\mathrm{ws}})$.

For the pair $\mathcal{G}^{\mathrm{h}}_{\mathrm{cs}}$ and $\mathcal{G}^{\mathrm{h}}_{\mathrm{me}}$ the number of parameters in the latter hypothesis is smaller than that of the $\mathcal{G}^{\mathrm{h}}_{\mathrm{cs}}$. Under similar reasoning as in Lemma B.1, we can claim that $Y \not\!\perp\!\!\!\perp X_l$ almost surely. The rest follows from established asymptotic behaviour of $\mathrm{BIC}^{\mathrm{ML}}_{\hat{Z}}$ as a special case of BIC, due to the decomposability property that $\mathrm{BIC}^{\mathrm{ML}}_{\hat{Z}}$ inherits from BIC. □

Using this result, we can extend the local consistency of $\mathrm{BIC}^{\mathrm{ML}}_{\hat{Z}}$ to its global consistency.

Corollary 3.4. *The latent-aware score* $\mathrm{BIC}^{ML}_{\hat{Z}}$ *is a consistent scoring criterion.*

Proof. By considering any sequence of appropriate single edge modifications between adjacent structural hypotheses as in Fig. B.2, we can extend the global consistency of BIC to that of $\mathrm{BIC}^{\mathrm{ML}}_{\hat{Z}}$ Chickering, 2002. □

C Implementation Considerations

We note that our main theory covers the Greedy Equivalent Search (GES) algorithm. In our implementation, however, we have used TOPIC [Xu et al., 2025], a more recent greedy score-based search that has similar guarantees to GES, and when similar requirements are met by the used score. Hence, we replace within TOPIC our proposed $\mathrm{BIC}^{\mathrm{EM}}_{\hat{Z}}$ score, to thus derive $\mathrm{TOPIC}_{\mathrm{BIC}}$, and here analyse the two algorithms.

We first assume access to the MLE oracle. Then, although the output of both algorithms lies on the domain of all CPDAGs over $\boldsymbol{X}$, $\mathrm{TOPIC}_{\mathrm{BIC}}$ builds on TOPIC, which is both asymptotically and practically more efficient than GES. Indeed, in each iteration, it first limits the candidate hypotheses from the set of all representatives of the Markov equivalence classes which perform a single-edge modification from the current best, to only those which differ with respect to the most likely modified source. Formally, the combination of these two steps are two subsequent maximisations over exactly the same domain (of all hypotheses with single edge modifications), only performed first over the possible sources, and then over the rest of the hypotheses, conditioned on the chosen source. Hence, at each iteration, the asymptotic greedy optimum is the same in both algorithms.

To see the asymptotical consistency, in the particular assumptions of our causal model, we treat two different cases. First, when no latent variable affects the result, $\mathrm{TOPIC}_{\mathrm{BIC}}$ would have similar ease to detect edge additions as in the case of TOPIC/GES. In the case that a the true structure is an Mixture

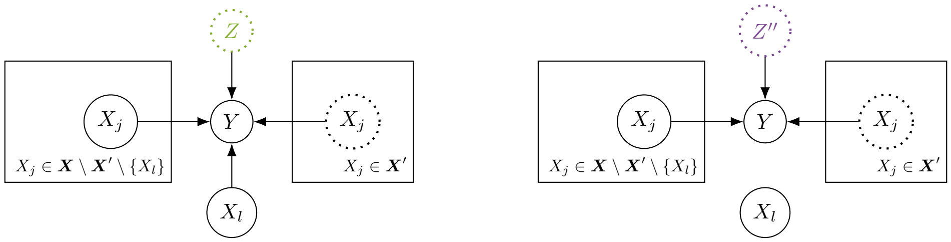
Z
X_j
Y
X_j
$X_j \in \boldsymbol{X} \setminus \boldsymbol{X}' \setminus \{X_l\}$
$X_j \in \boldsymbol{X}'$
X_l
Z''
X_j
Y
X_j
$X_j \in \boldsymbol{X} \setminus \boldsymbol{X}' \setminus \{X_l\}$
$X_j \in \boldsymbol{X}'$
X_l

(a) Correct Structure $\mathcal{G}^{\text{h}}_{\text{cs}}$

(b) Missing edge $\mathcal{G}^{\text{h}}_{\text{me}}$

Figure C.1: Decomposability of the MLR model in the intermediate stages of $\text{TOPIC}_{\text{BIC}}$. The so-far-undiscovered edges in $\boldsymbol{X}' \subseteq \boldsymbol{X}$ are akin to noise that affects both cases equally.

of Linear Regressions (MLR) model, we can consider the sequence of edge modifications that the $\text{TOPIC}_{\text{BIC}}$ algorithm would produce. Within this sequence, we can revisit the cases of Fig. B.2, and notice that when a subset $\boldsymbol{X}' \subset \boldsymbol{X}$ is not yet discovered in the structure of the algorithm, the effects of the so-far-undicovered variables $\boldsymbol{X}'$ can be seen as added noise, which equally affects an appropriate hypothesis $\mathcal{G}^{\text{h}}_{\text{cs}}$ and $\mathcal{G}^{\text{h}}_{\text{me}}$, as shown in Fig. C1.

Hence, intuitively, we expect a point at which one of the edges of the type $X_l \to Y$ would be added to the model, until all parents $\boldsymbol{X}$ will be discovered. Finally, we posit that the practical use of $\text{BIC}^{\text{EM}}_{\hat{Z}}$ in lieu of $\text{BIC}^{\text{ML}}_{\hat{Z}}$ is equally affecting both frameworks, as long as Conjecture 1 holds.

D Detailed Evaluation

Experimental Setup We give a more detailed description of our synthetic data generation here. In iteration $i \in \{1, \dots N_I\}$ of each experiment, we randomly sample a DAG $\mathcal{G}$ over $N_X := |\boldsymbol{X}|$ observed variables under an Erdős Rènyi model with edge density $p_{\mathcal{G}} \in [0, 1]$. In addition, we draw $N_Z := |\boldsymbol{Z}|$ latent mixing variables $Z_i \sim \text{Categorical}(\boldsymbol{\gamma}^i)$ with $Z_i \in \{1, \dots, K_i\}$, where we fix all $K_i =: K$ to the same hyperparameter K. We then sample a set of so-called mixing targets $\boldsymbol{T} = \{X_j \mid \exists Z_i : \text{La}_j = Z_i\} \subseteq \boldsymbol{X}$ where $X_j \in \boldsymbol{T}$ with probability $p_Z \in [0, 1]$. We distribute the effect of the N_Z mixing variables equally across these targets, resulting in $0 \leq i \leq N_Z$ many disjoint sets $\boldsymbol{T}_i = \{X_j \mid \text{La}_j = Z_i\}$. For example, we have $\boldsymbol{T}_1 = \{X_1, X_2\}$ and $\boldsymbol{T}_2 = \{X_4\}$ in Fig. 2.

To generate samples, we traverse $\boldsymbol{X}$ in topological order of the induced $\mathcal{G}$. For each X_j, we sample $\mathbf{B}_j = \{\boldsymbol{\beta}_{j1}, \dots, \boldsymbol{\beta}_{jK_i}\}$ coefficient vectors, where $\boldsymbol{\beta}_{jk} \in \mathbb{R}^{|\mathbf{Pa}_j|}$ for all $k \in \{1, \dots, K_i\}$ with $K_i = K$ if $X_j \in \boldsymbol{T}$ and $K_i = 1$ otherwise. We draw $\boldsymbol{\beta}_{jk} \in [-1, -\epsilon] \cup [\epsilon, 1]$ to avoid causal effects close to zero, and if possible also ensure that $|\boldsymbol{\beta}_{jk} - \boldsymbol{\beta}_{jk'}| > \epsilon$ for all pairs k, k' to create sufficient class separation, where $\epsilon = 0.25$ by default. We then draw S samples from a (mixture of) linear regression model(s) $(X_j | \mathbf{Pa}_j = \mathbf{y}) \sim \text{MLR}\left(\mathbf{B}_j, \gamma^j, \sigma^2\right)$, and standardize the resulting samples to generate an internally-standardized structural causal model (iSCM) [Ormaniec et al., 2024].

In the case studies, we consider a mixture of interventional datasets, as well as the flow cytometry dataset by Sachs et al., 2005 under the experimental setup in Wang et al., 2017. For both cases, we use the same scripts as in Kumar et al., 2024[2]. For the mixture of interventions, we have $N_Z = 1$ with $K = N_X + 1$ classes which defines a split into one observational and K interventional datasets. Under a so-called diagonal or atomic setting, one node at a time undergoes intervention, resulting in disjoint sets $\boldsymbol{I}_k \subseteq \boldsymbol{X}$, here with hard interventions that fix $\boldsymbol{\beta}_{jk} = 0$ if $X_j \in \boldsymbol{I}_k$. A similar structure applies to the real-world dataset with 5846 samples and known manipulations on 5 of the 11 variables, namely $\boldsymbol{I}_1 = \{\text{Akt}\}, \boldsymbol{I}_2 = \{\text{PKC}\}, \boldsymbol{I}_3 = \{\text{PIP2}\}, \boldsymbol{I}_4 = \{\text{Mek}\}, \boldsymbol{I}_5 = \{\text{PIP3}\}$.

Evaluation Metrics To evaluate the discovered number of mixing components and assignments, standard metrics in clustering evaluation are appropriate, where we show the v-measure and the Adjusted Mutual Information (AMI) as two examples (e.g., Vinh et al., 2010). We average each score over $\boldsymbol{X}$ since we can associate each variable X_j to a fixed assignment with K_i components if $\text{La}_j = Z_i$, else $K_i = 1$. To validate statements on *whether* observed variables are mixing targets,

[2] using the implementation of Mixture-UTIGSP at `https://github.com/BigBang0072/mixture_mec`

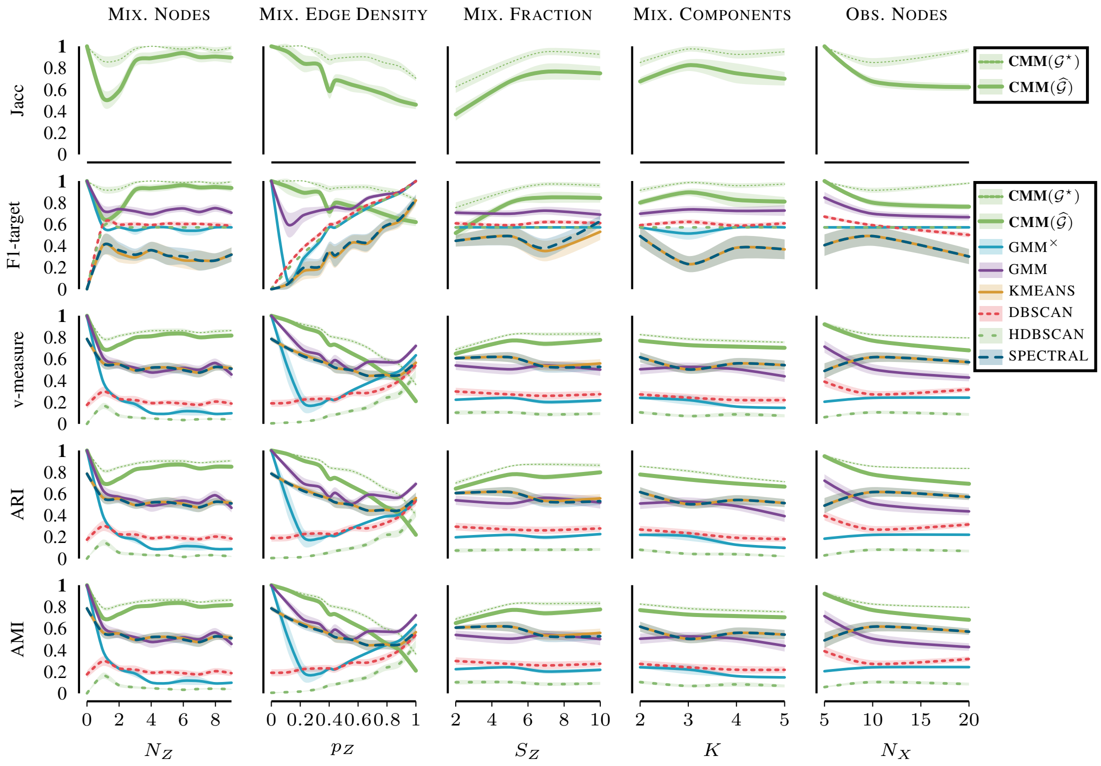

Figure D.1: *Discovering Mixing Structure.* In synthetically generated CMMs, we evaluate the quality of the recovered mixing structure, evaluating the affected observed variables (F1 (target)), variable sets affected by the same latent variable (Jacc) as well as per-node mixing assignments (AMI, ARI, v-measure).

we compute F1 scores (called F1-target) over the statement $X_j \in \boldsymbol{T}$ averaged over $\boldsymbol{X}$. To validate results on *which* mixing variables affect which mixing targets, we compute the Jaccard index (called Jacc) comparing the true sets $\{\boldsymbol{T}_1, \ldots, \boldsymbol{T}_{Z_m}\}$ to those returned by our algorithm.

We also compare the induced DAG $\mathcal{G}$ against the discovered DAG or CPDAG $\mathcal{G}'$. To give intuitive insight into correct vs. incorrect edge orientations, we show F1 scores over directed edge counts E in $\mathcal{G}'$ (called F1-dir), where we note that in the case of CPDAGs, we only count edges that are directed with certainty. As this is a simplistic score mainly included for illustrative purposes, we also consider classical distance metrics. A common distance measure for two DAGs or CPDAGs $\mathcal{G}, \mathcal{G}'$ is the Structural Hamming Distance (SHD). More suitable for graphs $\mathcal{G}, \mathcal{G}'$ with a causal interpretation are the scores proposed in Wahl and Runge, 2024. The *s/c-metrics* (S/C) are based on counting separation statements and comparing their validity in $\mathcal{G}, \mathcal{G}'$. Scalable variants thereof are the *separation distances* (SD) that associate each pair of separable nodes in $\mathcal{G}'$ with a separation set $\mathcal{S}$ under a given separation strategy, and validate whether $\mathcal{S}$ remains separating in $\mathcal{G}$. We report the SC (without randomization) and the SD (with the '`parent`' resp. '`pparent`' type), which are defined both when the output is a DAG or a CPDAG[3].

Baselines As our method is the only one to discover the full $\mathcal{G}^Z$, we show (i) AMI and F1-target scores over $\boldsymbol{X}$ for all clustering baselines and wherever applicable for Mixture-UTIGSP, (ii) metrics on $\mathcal{G}$ for all causal discovery baselines, and (iii) Jaccard scores over $\{\boldsymbol{T}_i\}_i$ only for our method. We note that we apply all baselines without optimization of their hyperparameters using their implementations available in the `causal-learn`, `causal discovery toolbox (cdt)`, `causalDisco` and `dodiscover` Python libraries. For all conditional-independence tests, we use the Fisher-Z test given the linearity of our functional model. We ran the evaluations on an 11th Gen Intel Core i9 CPU.

[3] using the implementation of the metrics at `https://github.com/JonasChoice/sep_distances`

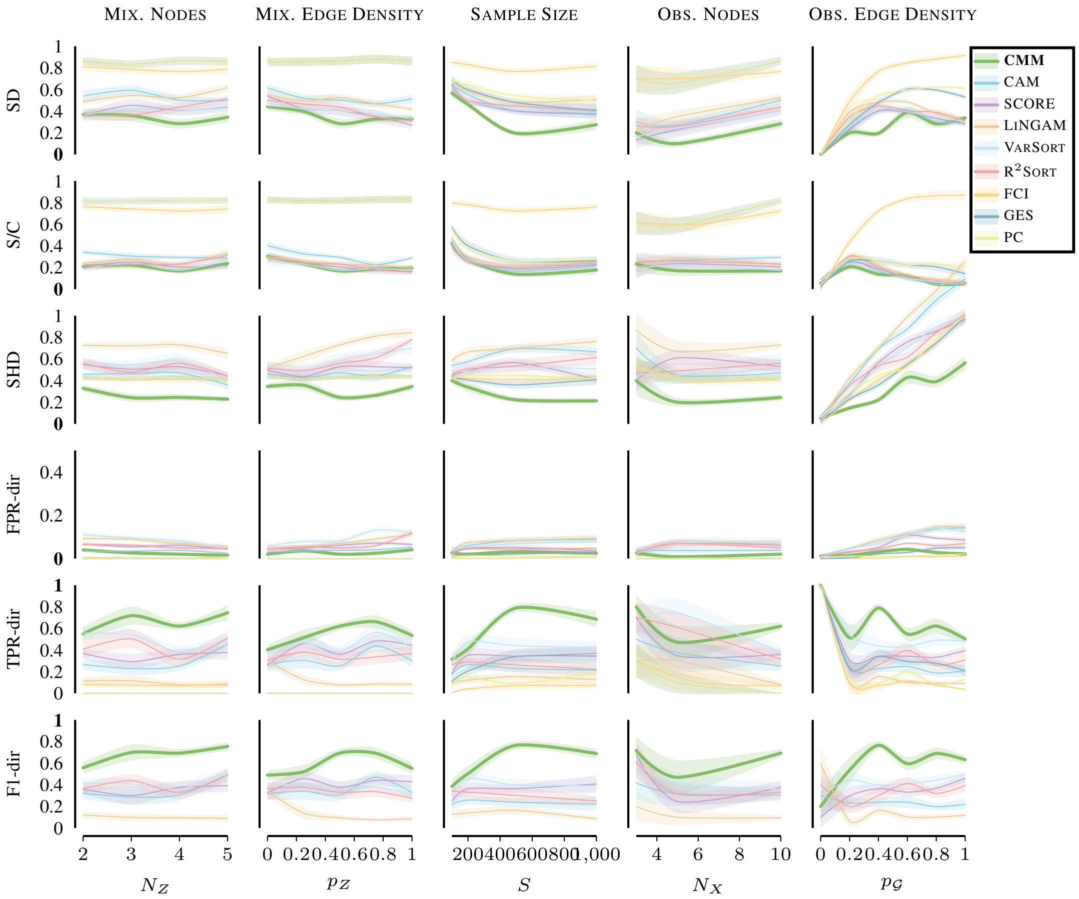

Figure D.2: *Discovering Causal Graphs.* In synthetically generated CMMs, we evaluate the quality of the causal DAG over the observed variables in terms of separation distances (SD, S/C), structural hamming distance (SHD) and directed edge counts (F1-dir, TPR-dir, FPR-dir).

Discovering Mixing Structure Fig. D.1 shows an extended variant of Fig. 4 in the main manuscript. The parameters are $N_X = 10, N_Z = 2, K = 2, p_Z = 0.4, p_{\mathcal{G}} = 0.4, S = 1000, S_Z = 5$, which are held fixed while changing one parameter of interest (columns in Fig. D.1), where we run $N_I = 10$ iterations for each parameter configuration. Different choices of the clustering algorithm besides the GMM, here shown in color for better readability, perform either worse on recovering targeted nodes (KMEANS, SPECTRAL) or mixing assignments (DBSCAN, HDBSCAN). We observe no noticeable differences between the clustering metric choices, so we report the AMI in the main manuscript.

Discovering Causal Structure Fig. D.2 shows an extended variant of Fig. 5 in the main manuscript. The parameters are $N_X = 10, N_Z = 4, K = 2, p_Z = 0.5, p_{\mathcal{G}} = 0.4, S = 500, S_Z = 5, N_I = 10$. All structural metrics (SD, S/C, and SHD) show stable performance of the CMM across the settings. The intuitive score TPR-dir furthermore suggests that our method performs well in distinguishing causal edge directions, improving as sample size S increases, and as the likelihood of mixing p_Z increases. In particular, the results suggest that "sparse" mixing $0 < p_Z < 1$ is most beneficial. We connect this to previous findings in the multi-environment setting [Perry et al., 2022] showing that identification of edge orientations is possible under the sparse mechanism shift hypothesis. This could inspire a future work direction generalizing this property from the multi-environment to the latent-mixed setting.

Discovering Interventional Mixtures Finally, Fig. D.2 extends Fig. 6 to show both mixing structure (Jacc, F1-iv) and causal structure (SD, S/C, SHD) discovery for the mixture of interventions. As a well-defined split into observational and interventional datasets exists for this setting, we also

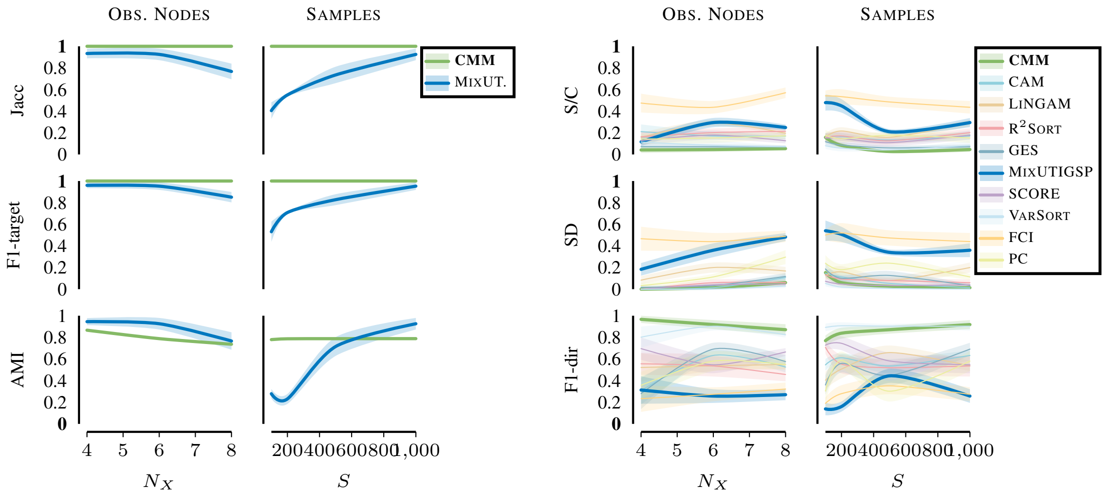

Figure D.3: *Mixtures of Interventions.* For data generated from an interventional mixture, we show the quality of discovered mixing (left) and graphs (right).

include Mixture-UTIGSP in the presentation (dark blue). The parameters $N_X \in \{4, 6, 8\}$ are as in Kumar et al., 2024, while we restrict the setting to up to $S = 1000$ samples, given that the true positive rates over $\mathcal{G}$ for the CMM (and VarSort) already approach 1 for $S = 1000$; we refer to Kumar et al., 2024 to see the performance of Mixture-UTIGSP with more samples. Compared to Fig. D.1, the CMM performs much better on discovering whether ($X_j \in \boldsymbol{T}$) and which ($X_j \in \boldsymbol{T}_i$) variables are mixing targets. A likely reason for this is the fact that the hard interventions $\boldsymbol{\beta} = 0$ create a more distinct separation than re-sampling of $\boldsymbol{\beta}$ with $|\boldsymbol{\beta}_{jk} - \boldsymbol{\beta}_{jk'}| > \epsilon$.

E Ablation Studies

As additions to our main experimental evaluation, we perform ablation studies on two questions.

(i) *Choice of Score-Based Algorithm.* We address the choice of the score-based causal discovery algorithm used together with the latent-aware BIC, showing GES alongside TOPIC.

(ii) *Effect of Latent Mixing Variables.* We take a closer look at how latent mixing affects causal discovery algorithms in practice. We hypothesize that spurious edges will appear between mixing targets, and study the extent to which the latent-aware BIC can prune these.

(iii) *Choice of Functional Forms.* Given that the results presented so far are restricted to linear settings, we test a proof-of-concept extension to nonlinear functional forms.

E.1 Choice of Score-Based Algorithm

	Causal Graph		
Metric	**CMM** (Topic)	**CMM** (GES)	GES
SHD	0.17 ± 0.01	0.31 ± 0.02	0.36 ± 0.04
S/C	0.13 ± 0.03	0.19 ± 0.03	0.26 ± 0.03
SD	0.17 ± 0.02	0.33 ± 0.03	0.48 ± 0.04

Table E.1: *Choice of Score-Based Algorithm.* We combine the CMM with different score-based algorithms (TOPIC, GES) as well as GES itself on causal discovery (cf. Fig. D.2).

While we used the latent-aware score $\mathrm{BIC}^{\mathrm{EM}}_{\hat{Z}}$ within the topological-ordering-based framework in the main evaluation, we can also use it within the GES algorithm, compared to GES with vanilla BIC. We compare these three variants in Table E.1 for the basic experimental parameters (as in

	Mixing Assignments (AMI)		
Function f	**CMM**-linear	**CMM**-natural-spline	GMM
linear	0.7624 ± 0.0378	**0.7659** ± 0.0296	0.3598 ± 0.0431
quadratic	0.6465 ± 0.0935	**0.7163** ± 0.0507	0.3116 ± 0.0452
cubic	0.5984 ± 0.0893	**0.6876** ± 0.0589	0.2841 ± 0.0554
exp	0.6345 ± 0.0860	**0.7025** ± 0.0544	0.3007 ± 0.0604
log	0.6628 ± 0.0849	**0.7100** ± 0.0527	0.3100 ± 0.0615
sin	0.6452 ± 0.0884	**0.7035** ± 0.0561	0.3144 ± 0.0603

Table E.2: *Choice of Functional Forms.* Under different generating processes f for the synthetic data, we compare the linear and a nonlinear instantiation of our model, in bold to indicate the best per-row model.

Fig. D.2). Regarding the choice of the algorithm, the topological-ordering-based variant (**CMM** (Topic)) appears to have better practical performance in our experiments. This experiment also confirms that regarding the score, $\mathrm{BIC}^{\mathrm{EM}}_{\hat{Z}}$ with MLR fitting (**CMM** (GES)) provides a benefit over plain BIC (GES).

E.2 Effect of Latent Mixing Variables

We are also interested in how exactly the presence of latent mixing variables influences the graphs $\mathcal{G}'$ returned by causal discovery methods unaware of mixing. As the latents $\boldsymbol{Z}$ introduce dependencies between the mixing targets $\boldsymbol{T}$, we presume that the reported $\mathcal{G}'$ will contain additional spurious (FP) edges.

In Fig. E.1 (light gray) we observe that the FPR in $\mathcal{G}'$ indeed increases as the probability p_Z of $X_j \in \boldsymbol{T}$ increases (shown for SCORE and CAM). Given this trend, we investigate whether we can correct the result by pruning any FPs that arise from mixing. Thus, we apply the CMM to each node X_j given its causes in $\mathcal{G}'$, fit an MLR, and use the $\mathrm{BIC}^{\mathrm{EM}}_{\hat{Z}}$ to remove any redundant parents of X_j under this model. This results in a graph $\mathcal{G}''$, also shown in Fig. E.1 (dark gray).

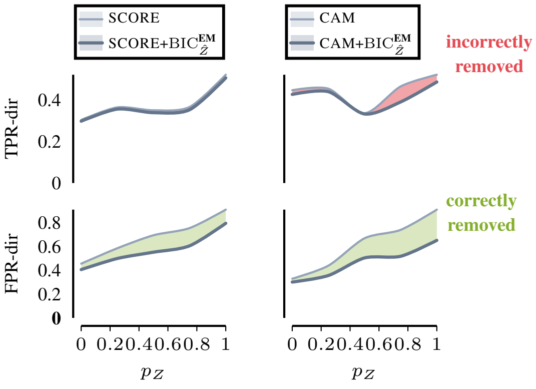

Figure E.1: *Effect of Latent Mixing.*

The shaded regions indicate the extent to which FP edges are removed correctly (green), respectively, TP edges are removed incorrectly (red). The $\mathrm{BIC}^{\mathrm{EM}}_{\hat{Z}}$ prunes some of the spurious and almost no causal edges. However, there still remain additional FPs in $\mathcal{G}''$ when p_Z increases. This is perhaps due to practical limitations of EM in estimating the correct mixing, leaving room for future improvements.

E.3 Choice of Functional Forms

While we consider it reasonable to limit the scope of our work to linear models, we also conducted a proof-of-concept case study to demonstrate the integration of nonlinear models.

For this, we replace the linear regression mixtures with nonlinear variants, specifically, a natural spline. We again use the EM algorithm to infer the mixture components and the BIC criterion to pick their number. Table E.2 shows how well we can reconstruct the mixture components (cf. Fig. 4 in the main text), measured by Adjusted Mutual Information (AMI) averaged over each node in 10-node graphs. We show the CMM with the MLR in as our main presentation (left) and the one with a mixture of natural splines (right) under different true generating functions (rows). The experimental setting corresponds to the same base parameters that we base Fig. 4 on.

The results match the expectations, where the models perform very closely in the linear case, but the MLR degrades in performance under nonlinearity. Replacing it with the mixture of splines allows covering the nonlinear cases reasonably well.

Conclusions We reach a similar conclusion from our questions in Sections E.1 and E.2: using the latent-aware BIC, we can expect not a substantial, but at least some improvement in causal discovery – be it via correcting the outputs of causal discovery algorithms (E.2), as an scoring criterion in GES replacing vanilla BIC (E.1), or similarly within TOPIC (Fig. D.2) – while in addition being able to discover the latent structure $\boldsymbol{Z}$ that can point us to subsamples of the data with a distinct causal generating process. Finally, the proof-of-concept experiment using nonlinear functional forms in Section E.3 also supports exploring our algorithm with more flexible regression mixtures.

F Limitations

One limitation regards the assumption of oracle MLR parameters; as a result, Alg. 1 is only consistent under appropriate conditions, such as a good-enough EM initialization regime, and otherwise should be viewed as a reasonable approximation to the problem. Studying the consistency of the estimates derived by the EM algorithm is a difficult problem, and the literature is limited to rather strict scenarios, which is why we cannot easily provide strict guarantees.

Given this, we can still note that the experimental evidence supports the connection we make in Conjecture3.5. There is also a reasonable mechanism that could theoretically explain the observed behaviour (asymptotically). Simply put, when the data truly follow the MLR model, it is more likely for our EM implementation to align with the oracle; when this does not happen, it is likely due to a faulty model, in which case our downstream process would anyways (asymptotically) reject the specific MLR hypothesis in favour of the correct alternative.

Furthermore, we limit the scope of the exposition mainly to linear additive noise models. While our guarantees for the latent-aware oracle BIC can in principle be transferred to a nonlinear setting, this would however require access to oracle mixture parameters, and the connection to estimates obtained using EM is less clear under nonlinearity. This point, while we supplement it with a small empirical analysis, requires a deeper theoretical analysis, which we postpone to future work.

References

Daphne Koller and Nir Friedman (July 2009). *Probabilistic Graphical Models: Principles and Techniques*. The MIT Press. ISBN: 978-0-262-01319-2.

Kenneth A. Bollen (1989). "Structural Equation Models with Observed Variables". In: *Structural Equations with Latent Variables*. John Wiley & Sons, Ltd. Chap. Four, pp. 80–150. ISBN: 978-1-118-61917-9.

Judea Pearl (2009). *Causality: Models, Reasoning and Inference*. Cambridge University Press.

David Maxwell Chickering (2002). "Optimal structure identification with greedy search". In: *Journal of machine learning research* 3.Nov, pp. 507–554.

Christopher Meek (Jan. 1997). "Graphical Models: Selecting causal and statistical models". In: DOI: `10.1184/R1/22696393.v1`. URL: `https://kilthub.cmu.edu/articles/thesis/Graphical_Models_Selecting_causal_and_statistical_models/22696393`.

Sascha Xu, Sarah Mameche, and Jilles Vreeken (2025). "Information-Theoretic Causal Discovery in Topological Order". In: *The 28th International Conference on Artificial Intelligence and Statistics*. URL: `https://openreview.net/forum?id=9pjJXQWYXc`.

Weronika Ormaniec, Scott Sussex, Lars Lorch, Bernhard Schölkopf, and Andreas Krause (June 2024). "Standardizing Structural Causal Models". In: *arXiv e-prints*, arXiv:2406.11601, arXiv:2406.11601. DOI: `10.48550/arXiv.2406.11601`. arXiv: `2406.11601 [cs.LG]`.

Karen Sachs, Omar Perez, Dana Pe'er, Douglas Lauffenburger, and Garry Nolan (2005). "Causal Protein-Signaling Networks Derived from Multiparameter Single-Cell Data". In: *Science*, pp. 523–9.

Yuhao Wang, Liam Solus, Karren Dai Yang, and Caroline Uhler (2017). "Permutation-based causal inference algorithms with interventions". In: *Proceedings of the 31st International Conference on Neural Information Processing Systems*. NIPS'17. Long Beach, California, USA: Curran Associates Inc., 5824–5833. ISBN: 9781510860964.

Abhinav Kumar, Kirankumar Shiragur, and Caroline Uhler (2024). "Learning Mixtures of Unknown Causal Interventions". In: *The Thirty-eighth Annual Conference on Neural Information Processing Systems*. URL: `https://openreview.net/forum?id=aC9mB1PqYJ`.

Nguyen Xuan Vinh, Julien Epps, and James Bailey (2010). "Information Theoretic Measures for Clusterings Comparison: Variants, Properties, Normalization and Correction for Chance". In: *Journal of Machine Learning Research* 11.95, pp. 2837–2854. URL: `http://jmlr.org/papers/v11/vinh10a.html`.

Jonas Wahl and Jakob Runge (Feb. 2024). "Separation-based distance measures for causal graphs". In: *arXiv e-prints*, arXiv:2402.04952, arXiv:2402.04952. DOI: `10.48550/arXiv.2402.04952`. arXiv: `2402.04952 [stat.ME]`.

Ronan Perry, Julius Von Kügelgen, and Bernhard Schölkopf (2022). "Causal Discovery in Heterogeneous Environments Under the Sparse Mechanism Shift Hypothesis". In: ed. by Alice H. Oh, Alekh Agarwal, Danielle Belgrave, and Kyunghyun Cho.